BRNO UNIVERSITY OF TECHNOLOGY

Faculty of Mechanical Engineering

Institute of Machine and Industrial Design

Ing. Ondřej Červinek

COMPUTATIONAL MODELS FOR NON-LINEAR MECHANICAL LOADING ANALYSES OF LATTICE STRUCTURES MADE BY LASER POWDER BED FUSION

VÝPOČTOVÉ MODELY PRO NELINEÁRNÍ ANALÝZY ZATĚŽOVÁNÍ MIKRO-PRUTOVÝCH STRUKTUR VYROBENÝCH TECHNOLOGIÍ LASEROVÉ FÚZE S PRÁŠKOVÝM LOŽEM

Shortened version of PhD Thesis

Branch: Design and Process Engineering

Supervisor: doc. Ing. Daniel Koutný, Ph.D.

CONTENT

1   INTRODUCTION

For fast energy absorption, e.g., in vehicle crashes, plastically deformed absorbers are used from specially shaped profiles made of mild steels and aluminum alloys. Their main purpose is the dissipation of kinetic energy during impact. Changes in shape and material allow tailoring of absorbers for a specific application. Their implementation in vehicle deformation zones increases the safety of the crew in case of an accident. However, customization of specially shaped profiles has certain limitations given by manufacturing technology.

Highly specialized applications use components precisely designed for a specific kind of deformation. In this category, a porous metamaterial with regularly repeated architecture can be included. These are, for example, aluminum foams or structures of honeycomb type. Metamaterials with internal architecture include a large volume fraction of pores (75-95%), which in the event of impact loading serves as a flexible damper and increases energy absorption capacity. However, these components are usually limited to a specific amount of energy absorbed and cannot be adapted for a wide range of deformation loads.

The solution provides structures with internal architecture produced by additive technologies, e.g., selective laser melting (SLM). Using SLM technology allows to efficiently combine multiple absorption characteristics by geometry changes like gradient volume fraction. The precise control of the structure shape enables tuning associated mechanical properties. As a result, components that protect passengers from collisions of varying intensity can be produced. Multifunctional absorbers with enhanced energy absorption capabilities can be designed for better adaptation to different types of car accidents. Furthermore, a large freedom of shapes in the internal architecture with a lightweight design can be obtained. Compared to metal foams, a wider range of metallic materials, such as titanium alloys (Ti_6Al_4V) or tool steels (1.2709), can be processed.

To effectively design and use lattice structures for energy absorption, it is necessary to mathematically describe their deformation behavior. This description can be done with analytical equations or, more efficiently, with computational software based on finite element methods (FEM). Research has shown that these structures have a specific type of behavior compared to bulk components. Therefore, to obtain a description of the behavior of the lattice structures, it is necessary to define specific input parameters of the material model, geometry and boundary conditions (contacts) involving non-linear effects. A precise numerical model that would reflect the influence of non-linearities of all types and at the same time the effect of imperfections and dynamic loading has not been the subject of studies yet. Therefore, this dissertation focuses on the development of a model that builds on existing knowledge in the field of FEM models and combines all of the aspects described above. It allows to obtain precise estimation of lattice structure properties under dynamic loading similar to those during vehicle crash. As a result, energy absorbers with a graduated deformation pattern can be achieved, which reduce the applied overload on the passenger.

2   STATE OF THE ART

Specially shaped profiles made of metal sheets and tubes are frequently used to absorb mechanical energy in deformation zones of vehicles in the transport industry. A suitable shaping of their geometry can increase the amount of energy that the absorber is able to dissipate during its deformation [1–3]. However, this procedure has limitations [4, 5]. Changing shape can rapidly increase stiffness. It leads to a stepwise change in force at the beginning of the plastic deformation, causing a force peak (stress peak respectively σ_{peak}; see Fig. 2-1) [6]. This force reaction peak is undesirable because it indicates step deformation deceleration, leading to a steep overload that can endanger the vehicle crew.
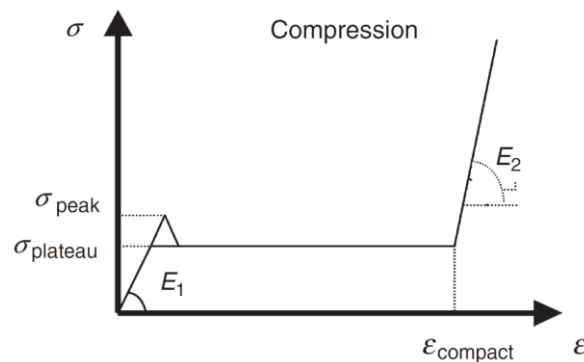

Fig. 2-1 Idealized stress-strain curve of lattice structure compression [6]

New applications combine these conventional absorbers with porous metamaterials [7–10] to increase their absorption capabilities and reduce the force peak [11, 12]. In the optimal course of deformation, a smooth transition from the elastic deformation to the uniform plastic deformation area can be observed. The plastic deformation should have uniform plateau character $\sigma_{plateau}$ and last until the compaction $\varepsilon_{compact}$ of the porous material [13]. This area, sometimes described as the area of progressive collapse, is most significant in active absorption. The engineering stress in this phase should be constant or possibly monotonically increasing [14]. It should be followed by a material densification area where the absorber is no longer able to efficiently dissipate energy. Some of the current metal foams approximate this model [15].

The development of additive technologies in recent years allowed the use of new types of porous materials that have potential in applications considering the absorption of mechanical energy [16–18]. These are lattice structures produced by SLM technology [13, 19]. Comparison of lattice structures with conventional porous materials such as extruded honeycomb and aluminum foams showed [20, 21] that they can achieve similar potential in the field of mechanical energy absorption. Furthermore, a wide range of materials can be used to produce these structures (SS316L [13], Ti_6V_4Al [22], $AlSi_{10}Mg$, $AlSi_7Mg_{0.6}$ [23, 24].

2

The geometry of the lattice structures can be controlled relatively precisely by several parameters and designed for the desired type of deformation or the amount of energy absorbed [17, 25]. It allows the tailoring of highly specialized parts which dissipate a specific energy shock with the required characteristics of deformation behavior. For an efficient estimation of the lattice structure properties, it is necessary to perform a detailed FEM analysis that includes quasi-static and dynamic loading [26, 27]. The model must contain knowledge about the properties of the structures obtained by mechanical testing [21]. It includes tensile and compression tests of the lattice structure material performed at several strain-rates [20].

Software that works with implicit and explicit FEM solvers is used for simulations of lattice structure deformation behavior [28–31]. These analyzes are based on the computational solution of the interactions of solid bodies or shock waves with structured blocks, which reflect the conditions of the experiments [32]. Using simulations allows to make changes of the geometry (material) model and observe their impact on the behavior of the structure with minimizing the production efforts.

2.1   Computational approaches and models of geometry

Luxner et al. [33–35] used computational approaches to simulate quasi-static compression of lattice structures. One of them used the geometry model described by beam elements with a quadratic interpolation function based on the Timoshenko beam theory. It allowed for large deformations, bending stresses, transverse shear deformations, and tensile stresses. The model was computationally cheap, but its accuracy was reduced due to several simplifications. Therefore, 1000 times increased Young's modulus in the near vicinity of nodes was required.

Labeas et al. [6] continued the development of two numerical models to predict of the dynamic deformation of the structure up to 5 m·s^{-1}. The first used beam elements BEAM 188 based on Timoshenko beam theory with quadratic shape function. It used a strut cross-section increased by 40% on 1/10 of the strut length to compensate for a higher material concentration around the strut junction points. The second type used homogenization by replacing the lattice structure with eight-node brick elements SOLID 164 with x, y and z degrees of freedom. They referred to translations, velocities, and acceleration suitable for explicit analysis [13].

The geometrical imperfections of the lattice structure were included by Ravari et al. [36], who used the Python 6.6.6 script to create a geometry model. The script split each strut into the required number of equivalent sections, which allowed to change the diameter independently for each section (see Fig. 2-2 (a)). The average diameters of the struts were changed according to the probability index assigned for each section of the strut (see Fig. 2-2 (b)). The diameter assignment was based on a pseudorandom distribution of the specific values range from previous measurements.

(a)   (b)
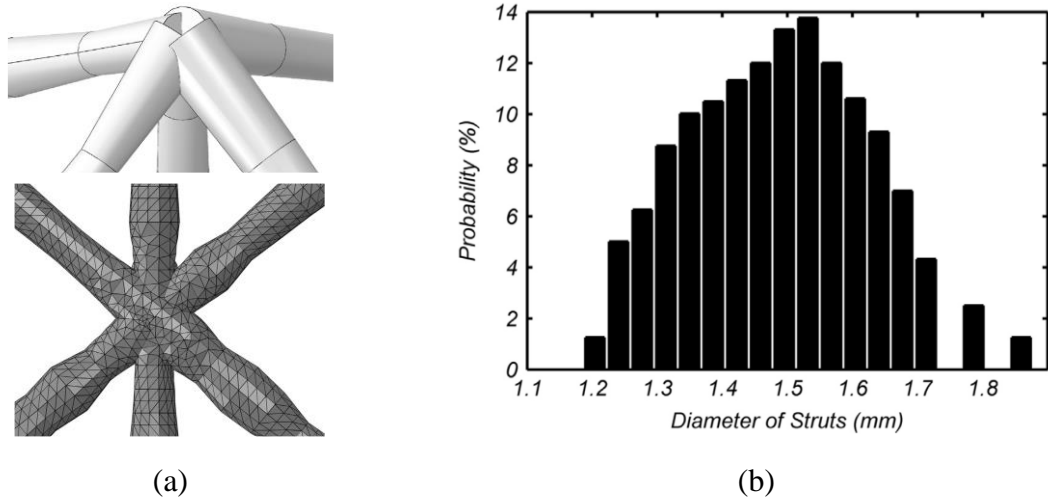
Fig. 2-2 (a) overlaps of the beam and solid element struts at nodes; (b) probabilities of strut diameter [36]

Dong et al. [37] tried to model the strut connections using the so-called joint stiffening concept. The proposed method was applied to determine the effect of joint connections and the stiffness of the struts. The segments at the ends of the strut were represented by joint elements (see Fig. 2-3). The middle segment represented the actual length of the strut reduced by the radii of the nodes.
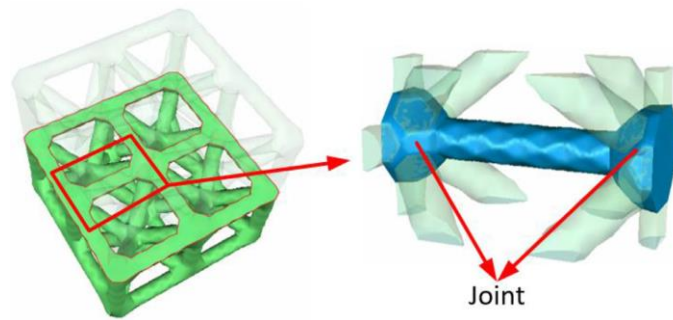
Fig. 2-3 The geometrical model of the joint stiffening element inside a lattice structure [37]

Geng et al. [38] reduced computational effort using beam elements (Timoshenko – shear flexible) but preserved the level of accuracy achievable for solid elements (C3D10 second-order tetrahedral). By replacing the beam elements of a specific unit cell in the middle of the structure with solid elements, a hybrid model was created. It allowed to make local changes in the geometry of the struts and closely monitor their effects on the stress response (see Fig. 2-4) [39]. To connect the beam elements with the solid elements, a bond called a multipoint constraint (MPC) was used, which reflected the actual conditions of the strut connection.

4
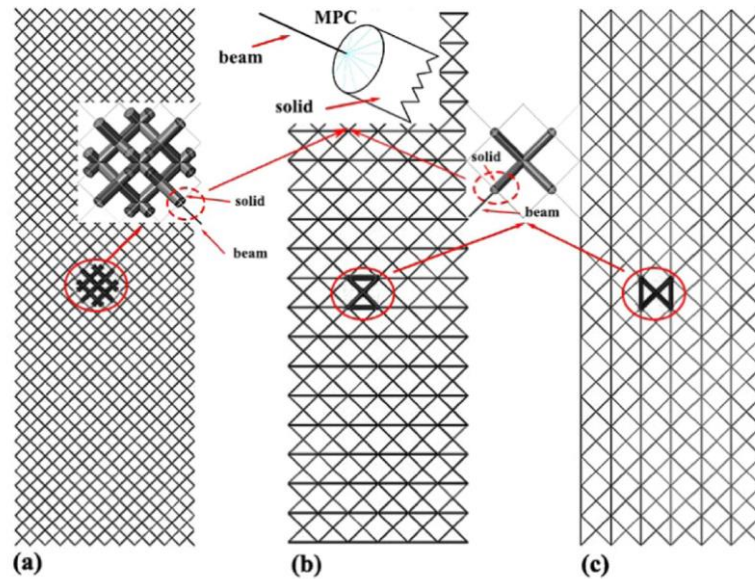
Fig. 2-4 Combined models of geometry (a) rhombic dodecahedron; (b) BCCz1; (c) BCCz2 [38]

To capture actual information about the geometry of the struts, Lei et al. [40] subjected the structures to micro-computed tomography (μ-CT) [41]. The results of μ-CT analysis showed that the diameter of the strut changed with its location in the structure and the manufacturing angle (similar to the findings of Koutny et al.) [42]. The boundary shape of the cross-section was fitted with a circle using the least squares method [43].

The models were prepared with an automatic Python script that served to generate geometry models using 3D B31 beam elements. The computational approach with pseudorandom assignment according to Gaussian distribution of diameters for individual segments similar to that used by Ravari et al. [36] was used. Furthermore, the strut diameter was defined based on reconstructed μ-CT scans and the fitting function with fast Fourier transformation.

Liu et al. [44] used an explicit Abaqus 6.14-1 module to predict the quasi-static loading behavior of the structure. A similar procedure was applied by Lei et al. [40] in a previous study. To guarantee the quasi-static response of the structure, the loading time was 10 times increased. Furthermore, two energy principles were followed according to the recommendations of the Abaqus developers [45]. The ratio of increase in artificial energy to internal energy was kept below 5% to guarantee minimization of the hourglass effect. Furthermore, the ratio of kinetic energy to internal energy was monitored with the same boundary criterion during the structure compression to maintain the dynamic effects at a negligible level. An optimum element size was determined according to the convergence test developed by Becker et al. [46].

Similar approach [47] for quasi-static compressive loading was introduced by Gümrük et al. [26]. The lack of stiffness in the vicinity of the vertices was compensated by increasing Young's modulus by about 50%, according to Luxner et al. [34]. The quasi-static loading simulation was created in the LS-DYNA explicit solver by an artificially increased loading rate while minimizing the effects of inertia. The criterion of quasi-static conditions was defined as the equal reaction forces between the loading and the bottom surface of the structure.

Lozanovski et al. [48] used the material model based on Yadroitsev et al. [49] to prepare simulations with models that used μ-CT scans. The μ-CT scanning was performed by thresholding and 3D reconstruction. The scanned data, including detailed information on the geometry of the struts, were divided into sections. The sections were intersected with a series of ellipses that approximated the actual shape of the struts (see Fig. 2-5) [50].
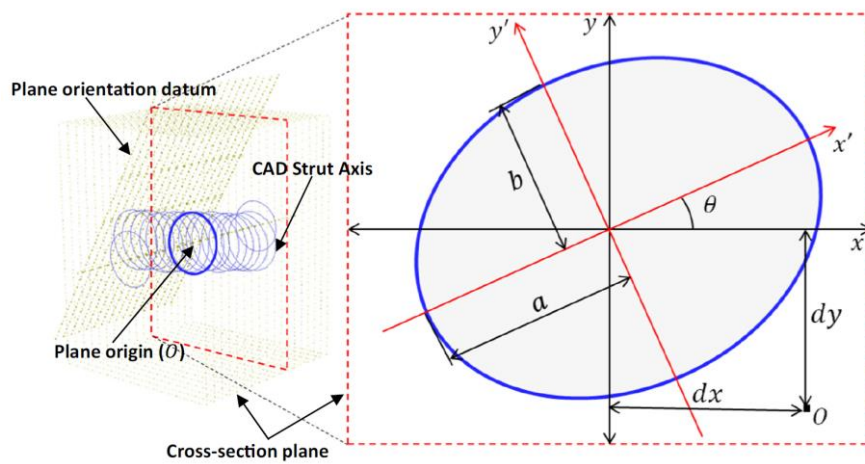
Fig. 2-5 Elliptical cross-section of the strut including variable parameters defining the dimensions and shape of the ellipse: *a*, *b* – radii of axes; d_x, d_y – vertical and horizontal displacement of the center of gravity with respect to the theoretical axis of the strut; *x'*, *y'* – rotated cross-section axis [48]

2.2 Models of material

Experimental testing of lattice structures showed that thin struts have different material characteristics compared to bulk components despite the same manufacturing procedure and the same parent material used. Tsopanos et al. [20] determined the properties of the parent material by tensile tests of single-strut samples. The tests required additional adjustment of the material model using simulation based on the lattice structure compression test [51]. Young's modulus of the parent material was parametrically changed until a good agreement was reached with the experimental and computational compression modulus of the structure.

Smith et al. [50] took the material properties of the Tsopanos study [52] and used reverse engineering methods to adjust the diameter of the strut in the simulation. At first, the initial diameter of the strut of 0.2 mm was chosen for simulation. Then the diameter of the strut varied until the compliance between the experiment and the simulation was achieved. The diameter of the struts near the nodes was increased to achieve a higher stiffness of the model, similar to the Luxner study [34].

Li et al. [27] used the elastic-plastic material model based on stress-strain curves of a single strut tensile test with a nominal diameter corresponding to the diameter of the structure strut. One end of the strut was captured during the tensile test by a high-resolution camera mapping the sample deformation. The result indicated a significant degradation of the material, probably due to the influence of pores in the struts [53].

Li et al. [54, 55] used input parameters of the $AlSi_{10}Mg$ alloy determined based on tensile tests of strut samples with the same nominal diameter as the structure struts diameter similar to Labeas et al. [13]. The geometry model in the simulation was created using a Python script. The FEM simulations were compared with analytical calculations based on the Gibson-Ashby [56] model and experiments. In addition, conventional tensile struts with a diameter of 5 mm were produced and tested. Despite equivalent production conditions and the same process parameters, significant differences were observed, similar to previous studies [14, 57]. These differences have been attributed to the effects of different heat transfers to thin struts and bulk material [54].

A similar approach was used by Labeas et al. [13], who prepared a bilinear elastic-plastic model of material with kinematic hardening Mat03 based on the quasi-static tensile test of struts with corrections. Corrections were determined using the calibration procedure suggested by Mines et al. [58]. For homogenized representation, the honeycomb type Mat26 was used. Each element behaved like six independent one-dimensional elements – three compressions and three shears. The stresses were a function of relative volume or volumetric strain. Later the material model was replaced by a non-linear orthotropic Mat40 [19]. The input parameters were based on the six independent non-linear stress-strain curves – three normal and three shear stresses.

Different approaches to modeling of lattice structure plasticity were compared by Harris et al. [59]. The curves of the actual stress σ_t depending on the logarithmic deformation ε_p were interpolated by the curves of the constitutive relations of plastic hardening (see **Chyba! N enalezen zdroj odkazů.**). Each of them represented a different stress-strain response. The parameters n_i and C_i obtained by interpolation were used to describe these relationships:

Hollomon [60]
$$\sigma_t = C_1 \varepsilon_p^{n_1} \ [MPa] \tag{2-1}$$

Ludwik [61]
$$\sigma_t = C_2 + C_1 \varepsilon_p^{n_1} \ [MPa] \tag{2-2}$$

Voce [62]
$$\sigma_t = C_2 - (C_2 - C_1)\exp(-n_1 \varepsilon_p) \ [MPa] \tag{2-3}$$

Ludwigson [63]

$$\sigma_t = C_1 \varepsilon_p^{n_1} + exp(C_2 + n_2 \varepsilon_p) \ [MPa] \quad (2\text{-}4)$$

Amani et al. [64] scanned the deformation process of the structures by in-situ and ex-situ X-ray tomography, capturing macroscopic changes in the structure geometry and local micro-porosity (see Fig. 2-6). The three-dimensional images were then used to create a simplified geometric representation of the structures, including manufacturing imperfections.
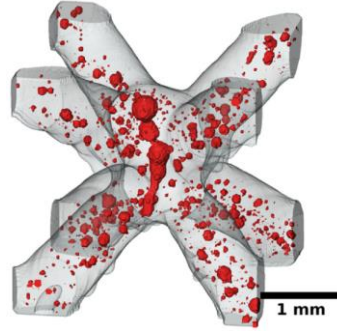
Fig. 2-6 Scan of basic BCC unit cell with red highlighted local pores [64]

The internal porosity information obtained by tomography was introduced via a Gurson-Tvergaard-Needleman (GTN) model of the material which assigned local porosity data to each element. The GTN model was based on von Mises yield criteria for ductile porous materials that included nucleation and growth of voids [65]. The basic equation of this model was defined as [66]:

$$\Phi\left(\sigma_{eq}, \sigma_y, \sigma_H, f\right) = \left(\frac{\sigma_{eq}}{\sigma_y}\right)^2 + 2fq_1 cosh\left(\frac{3q_2\sigma_H}{2\sigma_y}\right) - (1 + q_3 f^2) = 0 \quad (2\text{-}5)$$

where Φ is the yield function, σ_{eq} is the von Mises equivalent stress, σ_y is the yield stress, σ_H is the hydrostatic stress, q_1, q_2, and q_3 are calibrating parameters, and f is the void volume fraction in the matrix starting from an initial void volume fraction f_0 [67]. First-order volume tetrahedral elements were used to create a polygonal mesh for both approaches [64].

The model of material with constitutive law for the simulation of the lattice structure under dynamic loading was presented by Chen et al. [23]. Plasticity was represented by the constitutive law of simplified Johnson-Cook (J-C, MAT-98) [47] considering the deformation hardening effect and the strain-rate, but neglecting the effect of temperature:

$$\sigma = (A + B\varepsilon^n)\left(1 + Cln\frac{\dot{\varepsilon}}{\dot{\varepsilon}_0}\right) \ [MPa] \quad (2\text{-}6)$$

where σ is resulting stress value, $\dot{\varepsilon}_0$ is quasi-static strain-rate, $\dot{\varepsilon}$ is dynamic strain-rate, A is yield strength, B is hardening modulus, C strain-rate hardening coefficient and n is hardening exponent.

The full version of the J-C constitutive law was used by Grytten et al. [32] and Zmindak et al. [29, 68] to model the impact of high velocity on aluminum and steel plates at intermediate strain-rates 10^2-10^3 s^{-1}. The model was given by the equation, where isotropic hardening in which von Mises stress $\bar{\sigma}$ was expressed as a function of the equivalent plastic strain $\bar{\varepsilon}^{pl}$, equivalent plastic strain-rate $\dot{\bar{\varepsilon}}^{pl}$, a homologous temperature T^* and m coefficient of thermal softening [69]:

$$\bar{\sigma} = [A + B(\bar{\varepsilon}^{pl})^n]\left[1 + Cln\left(\frac{\dot{\bar{\varepsilon}}^{pl}}{\dot{\varepsilon}_0}\right)\right](1 - T^{*m}) \quad [MPa] \tag{2-7}$$

where $\dot{\bar{\varepsilon}}^{pl}/\dot{\varepsilon}_0$ is the normalized equivalent plastic strain-rate usually to 1 s^{-1}. The homologous temperature T^* is the defined as [68]:

$$T^* = \frac{(T - T_{room})}{(T_{melt} - T_{room})} \quad [-] \tag{2-8}$$

where T is the material temperature, T_{melt} is the melting temperature, and T_{room} is the room temperature. The equation for equivalent plastic deformation is given as:

$$\bar{\varepsilon}^{pl} = \left[d_1 + d_2 exp\left(d_3\frac{p}{\bar{\sigma}}\right)\right]\left[1 + d_4 ln\left(\frac{\dot{\bar{\varepsilon}}^{pl}}{\dot{\bar{\varepsilon}}_0^{pl}}\right)\right](1 - d_5) \quad [MPa] \tag{2-9}$$

where p is pressure and $d_1 - d_5$ are experimentally determined constants.

Gümrük et al. [18] continued with the model that considered the dynamic effect of the sensitivity of the parent material to the strain-rate in the area of plastic deformations. This dependence was introduced by means of the Cowper-Symonds (C-S) constitutive law supplemented with the isotropic elasticity behavior [1]. The basic equation can be described as follows [70]:

$$\frac{\sigma_o'}{\sigma_o} = 1 + \left(\frac{\dot{\varepsilon}_p}{D}\right)^{\frac{1}{q}} \quad [s^{-1}] \ pro \ \sigma_o' \geq \sigma_o \tag{2-10}$$

where σ_o' is the dynamic yield or ultimate tensile stress at uniaxial plastic deformation with strain-rate $\dot{\varepsilon}_p$. σ_o is the static stress and D and q are the constant material parameters.

To determine the input parameters of the constitutive law, the strut tensile tests were performed in the range of 10^{-3} s^{-1} to $6\cdot10^3$ s^{-1}. Low-velocity dynamic tensile tests were performed on a hydraulic device with single strut samples where significant oscillations of the system transmitted to the strain gauge occurred. This problem was described in a study by Fang et al. [8]. A modified Hopkinson device was used for high-velocity tensile testing (see Fig. 2-7) [71–73]. Special multi-strut bodies were used similar to those used by Dong et al. [37] for polymer materials. Based on the results, the stress, strain, and strain-rate values were obtained using the following equations [74, 75]:

$$\sigma = \frac{A_0 E_0}{A} \varepsilon_t(t) \quad [MPa] \tag{2-11}$$

$$\varepsilon(t) = -\frac{2C_0}{L} \int_0^t \varepsilon_t \, dt \quad [-] \tag{2-12}$$

$$\dot{\varepsilon} = -\frac{2C_0}{L} \varepsilon_r \quad [s^{-1}] \tag{2-13}$$

where $\varepsilon_t(t)$ and $\varepsilon_r(t)$ represented the transmitted wave and the reflected wave, respectively. A_0 indicated the cross-sectional area, E_0 the elasticity modulus of the bars, A the cross-sectional area of a micro-strut, L the size of the samples, and C_0 the elastic wave velocity given by equation [74]:

$$C_0 = \sqrt{\frac{E_0}{\rho_0}} \tag{2-14}$$

where ρ_0 is the density of the bars. The obtained values of dynamic yield strength or ultimate tensile stress for different strain-rates were fitted with curves. Constants D and q were determined as parameters of the polynomial function describing the fitting curve.
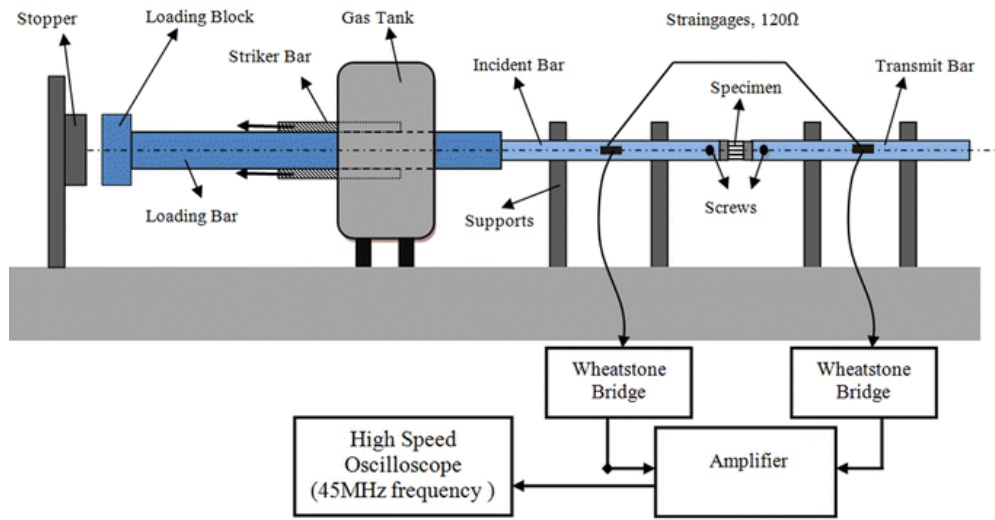
Fig. 2-7 Schematic of a Hopkinson device adapter for high-speed tensile tests [18]

Xiao et al. [22] used a similar evaluation of the split Hopkinson pressure bars test (SHPB, Kolsky bars) for dynamic compression of lattice structures (strain-rates up to 10^3 s^{-1}). Based on the one-dimensional stress wave theory and homogeneous hypothesis, nominal stress, strain and strain-rate were obtained using the following formula:

$$\sigma(t) = \frac{F_{input} + F_{output}}{2A_0} = \frac{E_B A_B}{2A_0} \left(\varepsilon_i(t) + \varepsilon_r(t) + \varepsilon_t(t) \right) \quad [MPa] \tag{2-15}$$

$$\varepsilon(t) = \frac{\Delta L}{L_0} = \frac{C_0}{L_0} \int_0^t \left(\varepsilon_i(\tau) - \varepsilon_r(\tau) - \varepsilon_t(\tau)\right) d\tau \quad [-] \tag{2-16}$$

$$\dot{\varepsilon}(t) = \frac{d\varepsilon(t)}{dt} = \frac{C_0}{L_0} \left(\varepsilon_i(\tau) - \varepsilon_r(\tau) - \varepsilon_t(\tau)\right) \quad [s^{-1}] \tag{2-17}$$

where E_B, A_B, and C_0 are elastic modulus, cross-section area and sound speed of the bars, respectively. $\varepsilon_i(t)$, $\varepsilon_r(t)$ and $\varepsilon_t(t)$ represent the elastic strain obtained for the incident wave, the reflected wave, and the transmitted wave. F_{input} and F_{output} represent the input and output force history at the bar-sample interface. L_0 is the initial length of the sample and ΔL is the relative displacement of the bar-sample interface.

2.3 Performance of lattice structures

To compare the performance of lattice structures with other porous metamaterials, the research teams developed their own metrics. Ushijima et al. [21] studied the main mechanisms that influenced the behavior of the structure, e.g., elastic and plastic buckling, axial and bending plasticity, rupture, etc. [76]. The influence was quantified using the plastic collapse strength $\sigma^*_{pl,BCC}$ defined as the initiation of fully plastic hinges [6] described by the equation:

$$\sigma^*_{pl,BCC} = \frac{4\sqrt{2\sigma_0}}{3}\left(\frac{d}{L}\right)^3 = \frac{\rho^*}{\rho_s} \cdot \frac{4\sqrt{6\sigma_0}}{9} \cdot \frac{d}{L} \quad [MPa] \tag{2-18}$$

where σ_0 is the flow stress, d is the diameter of the strut, L is the length of unit cell, and ρ^*/ρ_s is the relative density with ρ^* actual overall density of structure and ρ_s density of parent material. Mines et al. [16] continued to develop the analytical model to estimate the actual diameter of the BCC structure strut based on the weight. It allowed the detection of anisotropic imperfections related to changes in the geometry of related struts [26]. The calculated diameter of the struts is given as:

$$d = \sqrt{\frac{m_b}{\rho_p \pi N^3 L \sqrt{3}}} \quad [mm] \tag{2-19}$$

where m_b is the measured sample weight, ρ_p is the parent material density, N is the number of cells along the side length of the structure, and L is the unit cell length. A drop-weight test was used to compare the properties of structures made of SS 316L and Ti$_6$Al$_4$V by SLM with a honeycomb aluminum structure [77] and aluminum foam. To achieve a comparison of metamaterials with different volume fractions, the dissipated energy was divided by the average density of the sample – specific impact energy (SIE).

Tancogne-dejean et al. [14] evaluated energy absorption as the dissipated energy dependent on the relative density – specific energy absorption (SEA). The relative density $\bar{\rho}$ was defined by the ratio of the average density of the structure ρ and the density of the parent material ρ_s:

$$\bar{\rho} = \frac{\rho}{\rho_s} \quad [-]$$

(2-20)

SEA up to 0.3 strain was defined by the following equation:

$$\psi = \frac{W}{\rho} \quad [J \cdot m^{-3}]$$

(2-21)

with

$$W = \int\limits_0^{0.3} \sigma \, d\varepsilon \quad [J \cdot kg^{-1}]$$

(2-22)

where W is the work performed on the structure compression, σ is the axial stress and ε is the axial strain. If SEA of the structure was normalized by SEA of the fully dense material, the relative SEA was obtained, which was proportional to the relative density:

$$\frac{\psi}{\psi_s} = \frac{\rho}{\rho_s} \quad [-]$$

(2-23)

The assessed strength of the lattice structure increased by approximately 30% as the rate of relative deformation changed from 10^{-3} s^{-1} to 10^3 s^{-1}. This phenomenon was mainly attributed to the sensitivity of the parent material to the deformation rate.

Harris et al. [59] expressed the performance of the structure in terms of energy absorption efficiency described as:

$$\eta(\varepsilon_d) = \frac{1}{\sigma_m} \int\limits_0^{\varepsilon_d} \sigma \, d\varepsilon \quad [-]$$

(2-24)

where σ_m is the maximum nominal compressive stress in the range of $0 \leq \varepsilon \leq \varepsilon_d$ with ε_d indicating the maximum strain achieved. For quasi-static and dynamic loading, the geometry of the hybrid lattice structure significantly outperformed the lattice structures produced in previous studies [21, 78–80]. An increase in mechanical properties for the strength of the structure, SEA and absorption efficiency was observed. However, compared to the square honeycomb produced by additive technologies, these values were lower [81].

Similar metric to eq. 2-23 was used by Wang et al. [7] for the assessment of the energy absorption capacities of connectors with curved plates and aluminum foam. The stress and strain were replaced with force and displacement. Therefore, the energy absorption capacity of the connector was determined by integrating the force displacement as:

$$E_a = \int_0^{x_D} F(x)dx \quad [J]$$

(2-25)

Then the specific energy absorption was calculated as:

$$SEA = \frac{E_a}{m_{ct}} \quad [J]$$

(2-26)

where m_{ct} is total mass of aluminum foam and plates. The energy absorption efficiency was defined by:

$$\eta(x) = \frac{1}{F(x)H} \int_{x_y}^{x} F(x)dx \quad [-]$$

(2-27)

where $F(x)$ represents compressive force, H is height of aluminum foam and x_y is displacement at yield. Similar metric to eq. 2-21 was used by Xiao et al. [22, 82, 83]. The collapse strength metrics mentioned above [21] and energy absorption [14] were supplemented with specific plateau stress σ_{pl}^*. The specific plateau stress σ_{pl}^* was defined according to Gibson and Ashby [84, 85] for porous materials as follows:

$$\sigma_{pl}^* = \frac{\sigma_{pl}}{\rho} \int_{\varepsilon_s}^{\varepsilon_d} \sigma(\varepsilon)d\varepsilon/\rho \quad [MPa]$$

(2-28)

where σ_{pl} denotes plateau stress, ε_s strain related to collapse strength and ε_d=0.65 in the densification strain which corresponded to the origin of the rapid increase of stress. Modeling methods were taken from the Ozdemir study [25, 86].

Tancogne-Dejean et al. [14, 17] described the difference between quasi-static and dynamic loading by a coefficient called the dynamic increase factor (DIF). An approximately 30% stress difference was observed for the structure with 10% volume fraction and different strut tapering. The DIF values confirmed the findings of the previous study [22] for the same parent material.

Zhao et al. [87] determined the properties of a mathematically defined modification of the BCC structure using a triply periodic minimal surface (TPMS) representation. Smooth transitions between neighboring struts were achieved by mathematical shape definition, resulting in a more favorable distribution of the applied stress when loading the structure [88, 89]. The energy absorption of the structures was determined by numerical integration of the strain curve up to 50% deformation according to ISO 13314: 2011 [90]. The similar method up to 30% strain was used by Dejean-Tancogne et al. (see eq. 2-18) [14]. The same author [82] used a similar procedure for more TPMS structures.

3 ANALYSIS AND CONCLUSION OF LITERATURE REVIEW

The following section describes the analysis of knowledge based on research papers from the field of non-linear structural FEM simulations. It describes the most important modeling strategies and highlights their advantages and weaknesses.

3.1 Computational approaches

The aim of computational approaches was to explore the deformation pattern and estimate the behavior of the lattice structure. The first descriptions [33, 34] used beam elements based on Timoshenko's theory suitable for simulation of larger structures. The model considered large deformations, allowed for bending, transverse shear deformations, and stretching of the struts [35, 91]. The simulations were computationally cheap, but the beam representation required a stiffness correction introduced near the nodal points [26, 91]. Furthermore, it was recommended to modify the diameter and mass of the strut so that the beams in the vicinity of the nodes were equal to those of the real structure [13, 36, 50].

To represent the topology of the lattice structure in detail, a tetrahedron element model of geometry was created [26, 33]. This model provided a detailed description of the stress evolution across the strut cross-section. Its disadvantages were the high demands on hardware and computing times that limited size of the structure and scope of the simulation.

An alternative option was to use the so-called homogenized model of geometry [13, 19]. This concept used hexahedral elements with independent mechanical properties in each loading direction which were equal to the properties of the lattice structure. This approach allowed to solve computational problems of large structure deformations with omitting of complex interactions among struts in structures. On the other hand, its use for non-linear computations was shown to be significantly inaccurate.

One of the progressive approaches for the creation of a geometry model allowed the Python programming language [36]. Scripting made it possible to prepare code that divided struts of any cross-sectional shape into equivalent intervals with different diameter sizes [48, 88]. Individual diameters were assigned to the struts according to the experimentally measured probability intervals [36].

Another concept used the modeling and loading of a single strut enclosed in a lattice structure [37]. The approach was used to determine the effect of different joint connections of the struts on the stiffness of the lattice structure for solid or beam elements [41]. The similar method used in the following study [38] worked with models based on a combination of both types of elements. Some of the beam elements in the central cells of the loaded structure were replaced with tetrahedron elements. It provided a detailed overview of the development of stresses in the structure while maintaining low computational demands.

One of the methods used µ-CT to capture actual information about the shape of the strut surface, including imperfections [43, 88, 92]. The Python script was used to automatically generate a beam element model. Therefore, the actual distribution of imperfections was considered when the geometry model was generated. It was in contrast to the approach described above [36] that works with the random assignment of strut diameters to individual segments [36]. Another similar model captured the waviness of the struts that vary along their length using a series of elliptical cross-sections based on µ-CT scan measurements [48].

The explicit algorithm allowed to achieve longer duration of simulations considering large deformations until the structure densification [13, 55, 59]. Then metrics that compared the performance of the structure, such as energy absorption, were applied. To achieve a similar comparison for quasi-static simulations, some authors used explicit solvers to simulate slow events with an artificial quasi-static condition (see eq. 2-1) [26, 40, 43, 44, 54]. The ratio of artificially increased energy and internal energy, as well as the ratio of kinetic energy, and internal energy, was kept below 5%. Sometimes, the equilibrium of the force reaction was required on the loaded side and on the opposite side of the structure [26].

3.2   Models of material

The material model was represented by a mathematical description that determined the response of the material to mechanical excitations [14, 19, 22, 26]. Most of the initial approaches worked with the definition of a bilinear elastic-plastic model of material based on the tensile tests of the sample produced according to DIN standards [50]. Unfortunately, the material parameters obtained by the tests of these samples did not accurately represent the structure behavior [27, 54]. Therefore, the samples were replaced with thin long strut samples similar to struts of lattice structures [20]. Some authors directly used the same nominal strut diameter for samples and the corresponding structure [13, 54]. However, the resulting parameters were heavily underestimated, as single strut samples tended to fragile fractures caused by local defects. Therefore, these tests were supplemented with a quasi-static compression of the structure [50].

Measurement was usually considered as the reading of the elongation directly from the displacement of the head of the test machine [20]. However, this procedure did not consider slippage of a small circular sample in the jaws. An alternative type of measurement considered taking high-resolution images that captured the elongation of the test sample independently of the slip in the jaws [27]. The method allowed to do the post-processing correction of the measured data. The following methods offered the performance of tensile tests using samples composed of multiple struts joined to a single sample [18, 37]. This method seemed to be sufficiently accurate and representative to obtain the input parameters of a bilinear elastic-plastic model of the material (even for the J2-plasticity model) [14].

Furthermore, based on tensile tests and additional calibration, it was possible to construct a piece-wise linear (multi-linear) model with isotropic hardening [14]. This model allowed better capture of the development of stresses depending on the deformation of complex geometry. An even higher accuracy representation was achieved using a so-called homogeneous isotropic Levy-von Mises model, which combined ideal plasticity with isotropic strain hardening [17]. However, the model did not consider the effect of possible anisotropy, loading rate, kinematic hardening, and martensitic phase transformation [26]. Other strain hardening models that used different fitting parameters were developed by Hollomon (see eq. 2-1) [60], Ludwik (see eq. 2-2) [61], Voce (see eq. 2-3) [62], and Ludwigson (see eq. 2-4) [59, 63].

The most advanced model of the material reflecting the loading of the lattice structure was the model called porous plastic GTN (see eqs. 2-5) [64, 65]. The input values of this model were obtained by compression test of structures and X-ray tomography. The deformation process of the structure was captured by in-situ and ex-situ tomography showing macroscopic structural and local micro-porosity. A special procedure was used to assign local porosity properties to individual elements based on tomography images.

Even the most sophisticated material models from above-described did not consider the effects of dynamic loading. Therefore, some of these models were supplemented by other constitutive laws that considered the dynamic effect. One of these laws was known as Cowper-Symonds [71], which reflected the strain-rate sensitivity of the parent material (see eq. 2-10). The input values of this law were obtained by a dynamic tensile test of special multi-strut samples [18]. An example was Hopkinson Bars specially modified to perform a tensile test (see eqs. 2-11, 2-12, 2-13) [74, 75].

An alternative constitutive law was Johnson-Cook (see eq. 2-7) [29, 32, 55]. In addition to the effect of the strain-rate, this law also included the effect of material thermal softening of the material and the effect of large plastic strains (strain hardening) [93]. The law was supplemented with a corresponding damage criterion based on the formation of a crack in the material when the critical strain value was reached (see eq. 2-12). Its input parameters were obtained using the Taylor test [7, 28, 32, 94]. For lower strain-rates where neglect of the thermal effect was possible, a simplified version was used that considered only the strain-rate and the large plastic strain effect (see eq. 2-6) [22, 23, 47].

3.3 Performance of lattice structures

Non-linear FEM simulations used to estimate the deformation behavior of the lattice structures allowed to assess the energy absorption capabilities [22, 59]. Based on the software output data, the most efficient configurations were chosen [87]. It usually indicated the structures with the highest SEA (see eqs. 2-21, 2-26) [14, 16, 81]. Other key characteristics included the course of absorption or its efficiency (see eqs. 2-24, 2-27) [14, 59]. The preferred type was uniform energy absorption under constant stress during progressive collapse of the structure [19, 95]. A stable stress level without extreme fluctuations was especially required before the first plastic deformations occurred [1, 11, 96].

Stability of energy absorption was issue that arose (see eqs. 2-22, 2-25) [17] when fragile materials with low ductility were used for the production of structures (Ti_6Al_4V, $AlSi_{10}Mg$) [22, 87]. During structure compression, the struts were loaded with combined stress [97] with the highest stress concentration in the transition between the nodes and the struts. When the yield strength was exceeded, the strut-node interfaces started to rotate and were changed to plastic hinges. It caused cracks followed by fragmentation of the struts in the transition in the early stage of the deflection of the structure [87]. Therefore, it was appropriate to prevent this phenomenon by using materials with high elongation at break, e.g., SS 316L [14].

Except for the choice of parent material, the absorption of energy and the deformation pattern were fundamentally affected by the geometry of the basic elements of the structure called unit cells [98]. If these cells had high initial stiffness, usually caused by struts with an axis perpendicular to the loading direction, a step increase in applied stress occurred at the beginning of loading [13, 48]. The stress increased until buckling failure was achieved accompanied by plastic deformation of the struts (see eqs. 2-18; 2-38). This was followed by a rapid fluctuation of stress, usually associated with the collapse of several unit cells, unless the structure collapsed along the slip planes [99]. Therefore, it appeared to be efficient to use cells with lower initial stiffness and to further modify them to increase absorption efficiency [17, 22, 87].

4 AIM OF THE THESIS

This dissertation thesis aims at developing a computational model that represents the deformational behavior of mechanically loaded lattice structures produced by SLM technology primarily from stainless steel 316L. This model should include non-linearities arising from large deformations, the most significant manufacturing imperfections, and knowledge about the mechanisms of structural damage and failure for quasi-static and dynamic loading. To achieve the main goal of this thesis, the following steps must be taken:

- o Identification and execution of experimental procedures required for the determination of the mechanical properties of thin struts.
- o Identification and execution of procedures required to obtain actual geometry, including imperfections in the shape of the strut.
- o Development of non-linear quasi-static FEM analysis using solid and beam elements.
- o Calibration of the stiffness of the nodal connection for the beam element model to achieve compliance with the solid element model.
- o Implementation of geometrical imperfections related to change of strut cross-section shape and area to FEM simulation.
- o Determination of the dynamic behavior of the thin strut material and implementation of constitutive law reflecting the dynamic loading effects to the material model.
- o Verification of computational strategy for different loading velocities and structure topologies.

4.1 Scientific questions

Upon analysis and review of the literature, the following scientific questions were identified:

Q1 How do geometric imperfections of the cross-sectional shape and size affect the compression response of the lattice structures with a nominal strut diameter in the range of 0.6-1.2 mm?

Q2 How does the non-linear material model based on multi-strut tensile samples with stiffness corrections influence the deformation behavior of the lattice structure with nominal strut diameter in the range of 0.3-1.0 mm made of 316L stainless steel by SLM technology?

Q3 How does the implementation of strain-rate sensitivity into the model of material influence the behavior of the 316L stainless steel lattice structure under dynamic compression loading in the range of 10^2-10^3 s^{-1} strain-rate?

4.2 Hypothesis

Each scientific question was tested through working hypothesis formulated on the basis of the state of the art and previous research.

H1 Lattice structures produced by SLM technology show signs of anisotropic behavior due to the layer-wise building process that leads to non-uniform geometric imperfections arising on the struts during production [48]. The phenomenon is associated primarily with the increase in the load-bearing cross-section height of the strut, which leads to an increase in the mechanical properties in the direction of the building [16, 64]. As a consequence, a higher stiffness of the structure is expected to be observed [100]. The most significant imperfections are expected for struts with smaller diameters [54], where a high energy input related to the melted area is delivered during production. With increasing diameters of the struts, the significance of imperfections is expected to decrease. However, in the range of investigated diameters, these imperfections are not yet minimized to consider the mechanical properties change to be negligible [101, 102].

H2. LPBF scanning strategies applied to sample production create a different internal architecture for the subsurface and internal space of components with different material properties [20, 36]. The different proportions of subsurface and internal space for thin struts and DIN samples are expected to lead to a distinction in mechanical properties that cannot be neglected [16]. It can be assumed that performing a tensile test of samples that contain a series of thin struts with nominal strut diameter similar to the struts of the structure is necessary [18, 37]. Furthermore, due to simplified contact definition for the beam element model, it should be required to perform a compression test of the structure to reveal detailed characteristics of the deformation behavior [50]. Based on the findings, corrections of stiffness in the near area of the nodes have to be done to achieve the desired accuracy [33].

H3 Monitoring of the 316L stainless steel properties under dynamic loading showed an increased stress compared to quasi-static loading, even at a relatively low strain-rate about 10^2 s^{-1} [17]. A similar effect is expected in the case of thin strut structures produced by SLM technology, assuming the same parent material. The stress difference between quasi-static and dynamic loading should increase with increasing strain-rate. The dynamic effects such as the sensitivity of the parent material on strain-rate, micro-inertia, dynamic strengthening, thermal softening, or large deformation effects become amplified [16, 59, 103]. However, for low strain-rates, most of these effects have a negligible level compared to the strain-rate sensitivity, which becomes dominant [18]. Therefore, it is expected that the inclusion of this effect into the material model of the structure will significantly increase the level of dynamic stress for intermediate strain-rates (10^2-10^3 s^{-1}) and will improve the simulation accuracy [23, 74, 104].

4.3 Thesis layout

The main part of the dissertation thesis consists of three scientific papers published in peer-reviewed journals with an impact factor. The first paper [I.] focuses on answering the first scientific question of how geometric imperfections of shape and size affect the mechanical properties of the lattice structure. The second paper [II.] answers the second scientific question of how the input parameters of the non-linear material model based on multi-strut tensile samples with stiffness corrections influence the deformation behavior of the lattice structure. The third paper [III.] focuses on the third scientific question asking how the implementation of strain-rate sensitivity into the model of material influences the behavior of the lattice structure under dynamic compression loading.

I. VRÁNA, R.; ČERVINEK, O.; MAŇAS, P.; KOUTNÝ, D.; PALOUŠEK, D. Dynamic Loading of Lattice Structure Made by Selective Laser Melting-Numerical Model with Substitution of Geometrical Imperfections
Journal impact factor = 3.748, Quartile Q2, CiteScore = 4.7
Author's contribution: 20% (40%)

II. ČERVINEK, O.; WERNER, B.; KOUTNÝ, D.; VAVERKA, O.; PANTĚLEJEV, L.; PALOUŠEK, D. Computational Approaches of Quasi-Static Compression Loading of SS316L Lattice Structures Made by Selective Laser Melting. Materials, 2021, vol. 14, no. 9, p. 1-24. ISSN: 1996-1944.
Journal impact factor = 3.748, Quartile Q2, CiteScore = 4.7
Author's contribution: 55%

III. ČERVINEK, O.; PETTERMANN, H.; TODT, M.; KOUTNÝ, D.; VAVERKA, O. Non-linear dynamic finite element analysis of micro-strut lattice structures made by laser powder bed fusion. Journal of Materials Research and Technology, 2022, vol. 18, no. 1, p. 3684-3699. ISSN: 2238-7854.
Journal impact factor = 6.267, Quartile Q1, CiteScore = 5.9
Author's contribution: 65%

5 MATERIALS AND METHODS

To test hypotheses formulated on scientific questions, it was necessary to perform various experiments and FE analyses (see Fig. 5-1). The following section describes the equipment, methods, and experiments that were used to develop and verify a non-linear computational FEA of lattice structure loading, including dynamic effects and the most significant geometrical imperfections.
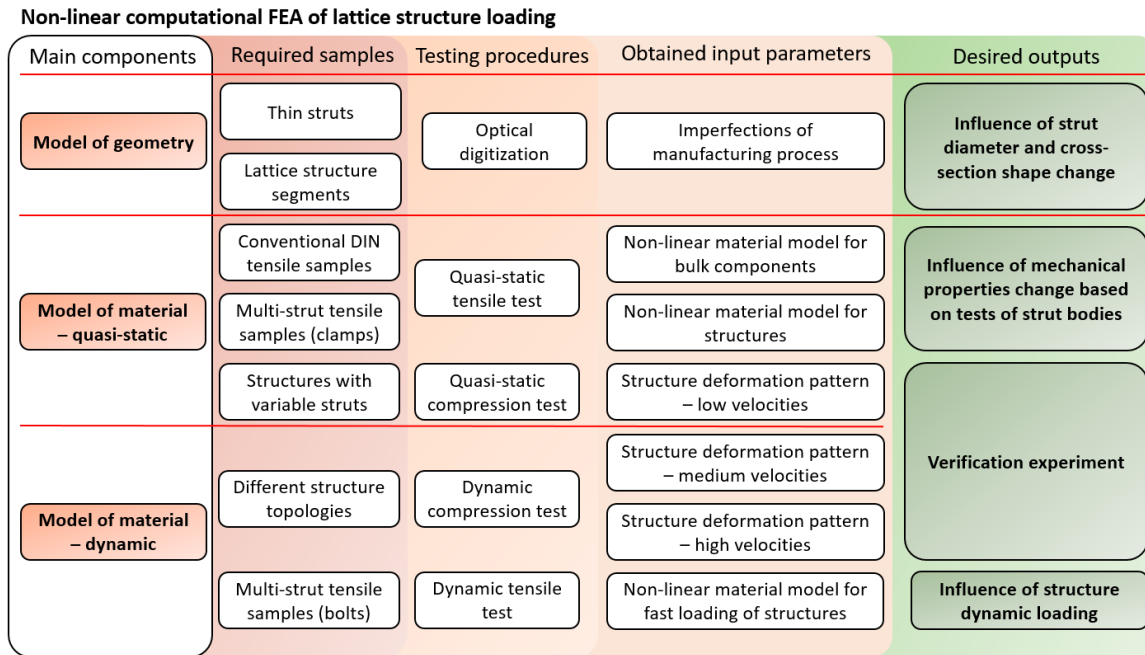
Fig. 5-1 Scheme of the most important methods and procedures used

5.1 Laser powder bed fusion

5.1.1 Process parameters

The samples were produced by SLM 280[HL] (SLM Solutions GmbH, Lübeck, Germany). The device was equipped with an YLR-400-WC-Y11 ytterbium fiber laser (IPG Photonics, Oxford, USA), which has a maximum power of 400 W with a Gaussian energy distribution. The process parameters were selected as a series of settings recommended by the machine provider for the SS 316L and $AlSi_{10}Mg$ materials (see Tab. 5-1). The scanning strategy was referred to bidirectional hatching with two contours. A 50 µm layer was used in combination with nitrogen atmosphere ($> 0.2 \%$ O_2).

Tab. 5-1 Basic process parameters of stainless steel 316L and $AlSi_{10}Mg$

Parameters		SS 316L	$AlSi_{10}Mg$	Unit
Platform temperature		100	150	°C
Borders	Laser power	100	300	W
	Scanning speed	300	600 (500)	mm·s^{-1}

Hatching	Laser power	275	350	W
	Scanning speed	700	1150 (930)	mm·s^{-1}
Fill contours	Laser power	150	250	W
	Scanning speed	400	555	mm·s^{-1}
Hatch distance		120	170 (150)	μm

Note: Values in brackets indicate parameters based on previous research used in the study.

5.1.2 Powder material

SS 316L and AlSi$_{10}$Mg supplied by TLS Technik GmbH (Bitterfeld, Germany) were selected for sample production. Their chemical composition (see Tab. 5-2) was close to that of the materials produced by SLM Solutions. The particle distribution before the first recycling cycle was Q_{10}=10.07 μm, Q_{50}=29.44 μm and Q_{90}=48.21 μm for steel and Q_{10}=25.2 μm, Q_{50}=40.7 μm and Q_{90}=58.0 μm for AlSi$_{10}$Mg.

Tab. 5-2 Result of chemical analysis of stainless steel 316L and AlSi$_{10}$Mg powders

SS 316L

Elem.	Fe	C	Si	Mn	Cr	Mo	Ni
wt-%	Bal.	0.03	0.8	1.8	17.5	2.2	11.3

AlSi$_{10}$Mg

Elem.	Al	Si	Mg	Fe	Ni+Cu	Other
wt-%	Bal.	9.8	0.35	0.14	<0.02	<0.1

5.1.3 Samples

Sample models were prepared in Inventor software (Autodesk, San Rafael, Californie, USA). Assignment of process parameters and data slicing was performed in Magics software (Materialize, Leuven, Belgium).

Single struts for optical digitization – were manufactured as 20 mm long distributed in the corners of the platform. The struts were manufactured with the same nominal diameter as the structure struts that cover all manufacturing angles of the struts in the structures.

Samples for tensile test (quasi-static, DIN 50125:2009-07) – to compare mechanical properties with thin struts, conventional tensile samples were produced with a manufacturing angle of 90°. The effect of surface and subsurface porosity was eliminated by machining.

Samples for tensile test (quasi-static, multi-strut) – consisted of 12 parallel struts with a length of 28 mm in an arrangement of 3 x 4 struts [105]. The multi-strut configuration was supposed to prevent a local weakening of the sample caused by pores in the strut that occur during production [18, 37]. The samples were designed with a nominal strut diameter of 0.6 mm, which was further considered as a reference [54].

Samples for tensile test (dynamic, multi-strut) – were manufactured in a configuration similar to multi-strut samples for quasi-static tests. The length of the struts was preserved, but the arrangement of the struts and the fastening part was adjusted to the Hopkinson device (2 x 6 struts configuration) [18, 37].

Structures for compression test (quasi-static, dynamic) – were designed as lattice structure cubes of the BCC or FCC based type [3, 26, 28], their combinations, and modifications with vertical struts [5, 98, 105, 106]. The dimensions of the structures were 20 x 20 x 20 mm with a unit cell side length of 4 mm. Due to the equivalent width to height dimensions, it was possible to observe whether slip planes occur on the sample diagonals during the pressure test [107].

5.2   Model of geometry

To obtain actual dimensions of the struts, the samples were digitized (see Fig. 5-2) after production with a blue light projection scanner ATOS Triple Scan (GOM GmbH, Braunschweig, Germany) [101, 108]. The scanner was equipped with MV170 optical lenses calibrated according to the VDI/VDE 2634 standard. Before scanning, the samples were coated with antireflective titanium dioxide [109]. The resulting 3D scans were evaluated using GOM Inspect (SR1, GOM GmbH, Braunschweig, Germany) [99, 110–112].

(a)   (b)
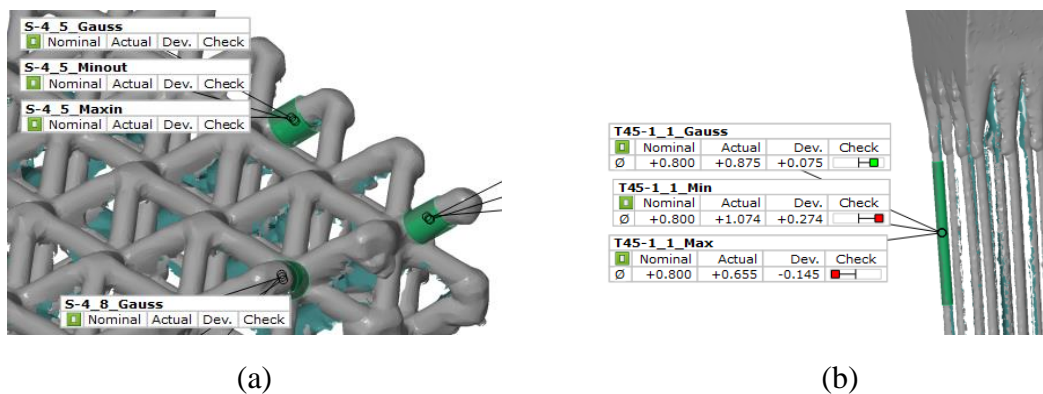
Fig. 5-2 Example of strut part selection for inspection – (a) on structure; (b) on tensile sample

The strut scans of were divided into sections using a semi-automated GOM script. These sections were intersected with simple geometric shapes such as a circle or ellipse, which were used to approximate the actual shape of the strut [48]. Based on the simplified shapes, geometry models were created in the FEM software.

After production, the structures were weighed with Sartorius MA35 (Sartorius, Göttingen, Germany). According to the measurement, an estimation of the actual volume fraction was made using eq. 2-19. Together with information on the strut dimensions, it was possible to approximately calculate the porosity and/or the amount of powder aggregated on the struts [16].

5.3 Model of material

5.3.1 Determination of mechanical properties

To estimate the behavior of the lattice structure under mechanical loading considering plastic deformation, it was necessary to perform experiments with a thin strut material.

Material properties (quasi-static) – to obtain material properties of stainless steel for quasi-static loading a uniaxial test on a Zwick Z250 (ZwickRoell GmbH & Co. KG, Ulm, Germany) was performed at strain-rate 10^{-3} s^{-1} (see Fig. 5-3). The tests were performed as compression of lattice structures (see Fig. 5-3 (a)) and tension of standard DIN and multi-strut tensile samples (see Fig. 5-3 (b)).

To determine the engineering stress-strain curves of multi-strut samples, the force reaction was divided by the overall cross-sectional area of the struts in the sample determined by optical digitization before testing. True stress-strain curves were determined using FEA. Based on the compression test results, a correction of stiffness in the near area of the nodes was made for the beam element model.

(a)   (b)
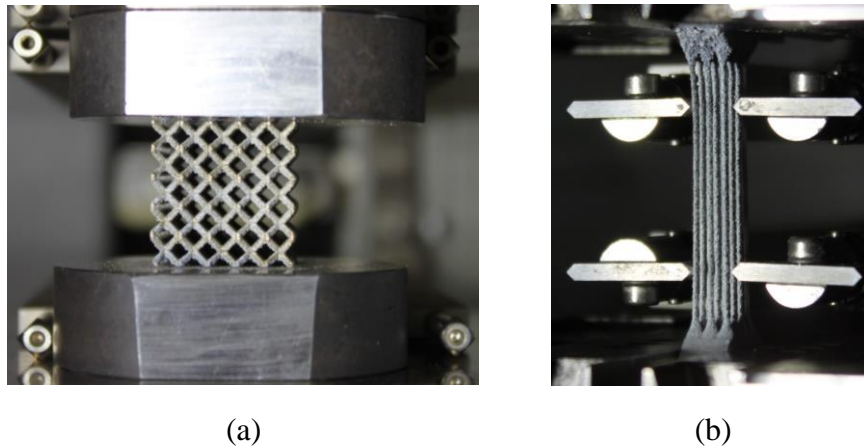
Fig. 5-3 Mounting of the samples in Zwick – (a) compression test; (b) tensile test

Material properties (dynamic) – were carried out using modified split Hopkinson tensile bars (SVS FEM, Brno, Czech Republic) to determine the mechanical properties of SS 316L under dynamic loading [18, 59]. The initial loading velocity was 30 m s^{-1} (equal to approx. 175-250 s^{-1}). The samples were attached between the bars of the device using a bolt connection. Semiconductor strain gauges EP140-3-35-G (VTS Zlín s.r.o., Zlín, Czech Republic) with a nominal resistance of 350 Ω, a grid length of 3 mm, and a k-factor of +140 were placed in pairs in the middle of both bars. The signal emitted from the Wheatstone bridge was strengthened with amplifiers and further recorded with a high-speed oscilloscope (recording frequency of 10 MHz). The signals from the gauges were evaluated assuming uniaxial stress wave theory in the form of engineering stress σ according to eq. 2-11, strain ε according to eq. 2-12, and strain-rate $\dot{\varepsilon}$ according to eqs. 2-13, 2-14 [29, 71].

5.3.2 Constitutive law

The model of material was defined as a non-linear elastic-plastic model [5] based on tensile tests of multi-strut samples (see Tab. 5-3). For quasi-static simulations, the behavior of the material after exceeding the yield point was described as linear isotropic hardening [13]. Unlike the Grytten study [32], the model was not supplemented with a material failure criterion, because SS 316L was ductile with high elongation at break and showed no signs of strut fragmentation even for large deformations [19, 26].

Tab. 5-3 Parameters of non-linear model of material

Parameters		Value	Unit
Isotropic elasticity	Density	7750	kg·m^{-3}
	Poisson's ratio	0.3	-
	Young's modulus	94	GPa
Bilinear plasticity	Yield strength	338	MPa
	Tangent modulus	787	MPa
Hollomon plasticity	Strength coefficient	481	MPa
	Hardening exponent	0.0656	-
Cowper-Symonds	*D*	80737	s^{-1}
	q	5.0075	-

The dynamic properties were described using a Cowper-Symonds constitutive law (see eq. 2-10) that considered the effect of the strain-rate, which was described for lattice structures by Ahmad et al. and Gümrük et al. [18, 113]. The law was combined with plasticity description using the Hollomon equation (see eq. 2-2) [59, 60].

5.3.3 Verification experiments

In order to verify the computational model at different loading rates, a series of experiments was performed and compared to FEA.

Quasi-static compression (strain-rate approx. 10^{-3} s^{-1}) – was performed as a compression test of lattice structures on Zwick described in section 5.3.1.. They were placed without fixing between the plate adapters of the device. The lower adapter was fixed on a movable bar in a vertical direction, and the upper adapter was mounted on a static joint connection to allow slight tilting.

Dynamic compression (strain-rate approx. 10^2 s^{-1}) – was performed as a drop-weight test on the impact tester (Impactor 2.1, BUT, Brno, Czechia) with maximum weight 13.45 kg [114, 115]. For these parameters, a crosshead was able to achieve a drop velocity of approximately 3.5 m·s^{-1} [68], equivalent to an impact energy of 60.5 J [16, 42, 88]. The device was equipped with a Phantom V710 high-speed camera (Vision Research, Wayne, New Jersey) and a strain gauge XY31-3/120 (HBM GmbH, Darmstadt, Germany). The strain gauge measured the reaction force, whereas the high-speed camera measured the position of the marker on the falling head to capture the deformation. A strain gauge signal was recorded using the Quantum MX410B data acquisition system (HBM GmbH, Darmstadt, Germany). The high-speed camera was recorded using Phantom Camera Control software version 3.5 (Vision Research, Wayne, NJ). Both records were compounded and evaluated in MATLAB R2021a software (MathWorks, Natick, Massachusetts).

Dynamic compression (strain-rate approx. 10^3 s^{-1}) – was performed on a Hopkinson device similar to that described in Section 5.3.1.. The device was based on the principle of moving bars toward each other, causing high-speed dynamic compression of the structures, as described by Nolting et al. [71, 74].

5.4 Computational approaches

Non-linear simulations of structure compression were created in the ANSYS Workbench software (Ansys Inc., Canonsburg, Pennsylvania, USA). Geometries for solid element models were created in the Inventor software. For beam element models, APDL and later Python script API v19 were used. The quasi-static simulations were prepared in a module called Static Structural using the Mechanical solver, while the dynamic simulations were prepared in the module Explicit Dynamics [54, 87] using the AUTODYN solver. Both types of simulation, quasi-static and dynamic, were prepared using two different approaches.

The first used solid tetrahedron elements type SOLID 187 with quadratic base function for discretization of modeled geometry. The model was considered as a reference and was used to simulate the loading of smaller structures and mild non-linearities. The second used beam elements type BEAM 189 based on Timoshenko's beam theory to create more extensive parametric studies. In this model, the stiffness of the elements in the vicinity of the nodes was modified according to the experiment and the solid element model to simulate the real contact of the struts (see Fig. 5-4) [34]. Furthermore, both types of models were subjected to a mesh sensitivity study to determine the appropriate number of elements to divide the strut length or its cross-section [14, 33, 50].

The structure was placed between rigid plates with artificially increased stiffness that represented surfaces of static support and deformational member similar to the experiment. For the discretization of both plates, shell elements of SHELL 93 type were used [44, 64].

Subsequently, frictional contacts that allowed sliding and separation on the target surface were defined at the interfaces of the deformation member-structure and the structure-static support. Tabular values for the steel-steel contact for both static and dynamic friction coefficients were considered. In the next steps, the boundary conditions, load velocity, and other computational settings were defined according to the specific purpose of the task.
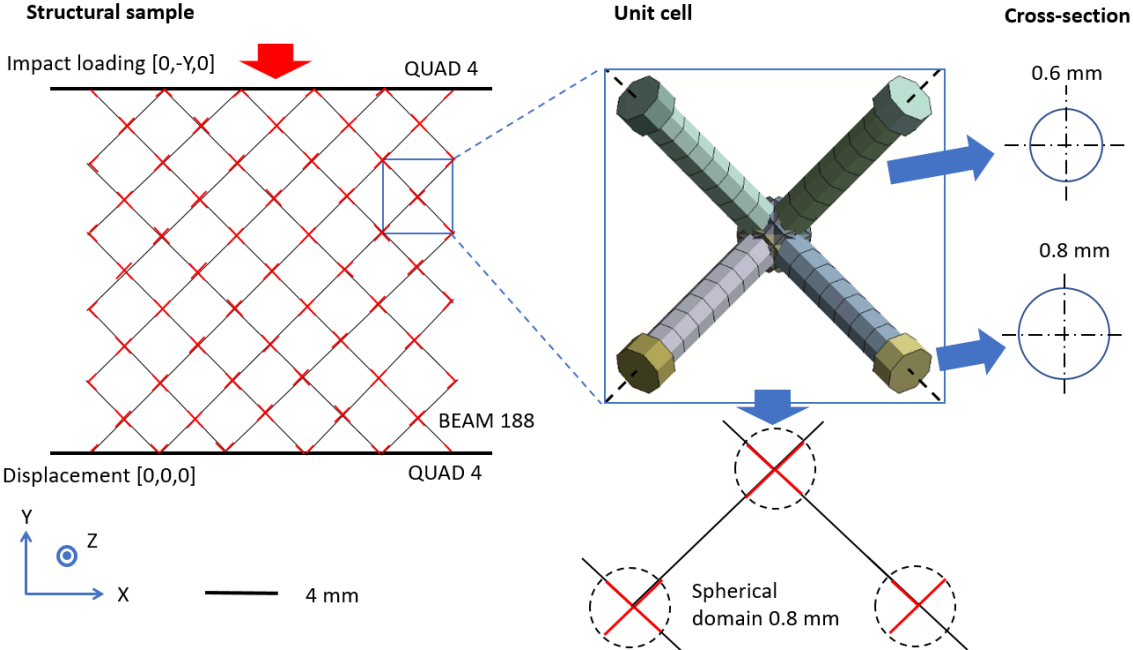

Fig. 5-4 Beam element model of BCC lattice structures with stiffness corrections and diameter changes

6 RESULTS AND DISCUSSION

The following section presents a summary of the most important results, especially in the field of non-linear computational modeling strategies that involve quasi-static and dynamic loading of lattice structures.

6.1 Research paper I

The key findings of Research Paper I were related to the geometry model. Attention was paid to a novel approach to include geometrical imperfections of the manufacturing process. The proposed methodology workflow was based on optical digitization of structure segments after the manufacturing process. The scanned struts were cut in several cross-sections and interlaced by several simplified shapes of circle and ellipse. This step allowed to accurately find the actual cross-section shape and its dimensions. Simplified shapes were used to make an equivalent comparison of geometries and create models suitable for FEM analyzes.

In the paper, the BCC lattice structure made of aluminum alloy $AlSi_{10}Mg$ with different parameters was investigated using an impact test and corresponding FEM analysis. In the first step, digitization of the structure segments was performed with a nominal strut diameter of 0.8 mm (section 5.2.). After digitization cross-sections were done in the mid-length of chosen struts. These cross-sections formed significantly irregular shapes similar to a water drop. In the next step, they were interlaced with circles according to several governing rules: maximum inscribed, minimum circumscribed, and circle with Gaussian distribution (with three-sigma accuracy). Additionally, an elliptical approximation of the actual cross-sectional shape was included because it better approximated the shape of the water drop.

The measurement results were consistent (0.94±0.08 mm for the circle with Gaussian distribution), but the different governing rules of the cross-sectional approximation showed significant differences in the measured diameters. The largest differences were observed for the diameters of the maximum inscribed and minimum circumscribed circle diameters (0.74±0.08 mm for the maximum inscribed circle and 1.25±0.17 for the minimum circumscribed circle). The result was attributed to the significant non-circularity of the measured sections (average minor/major axis ratio 0.71). Therefore, it was decided to compare experiment with FEM simulations for nominal geometry, geometry created with Gaussian distribution and elliptical cross-section. It allowed to assess the influence of imperfections independently.

The results were compared in terms of force reaction, duration of deformation, and deformation pattern. Initial comparison of experiment and simulation with nominal geometry of struts showed a significant underestimation of deformation resistance. The geometry was, therefore, modified according to the measurements, and the simulation was recalculated. It was shown that simulation considering the cross-section with circular Gaussian distribution achieved lower values of force reaction at the beginning of the plastic deformation compared to the experiment (approx. 12% difference). In addition, the duration of the deformation differed about 21%. In contrast, geometry created with elliptical cross-section achieved a good agreement of the force reaction compared to the experiment (approx. 2% difference). The comparison also showed a similar deformation pattern.

In the next step, a similar optical measurement and experimental testing procedure was performed for structures with nominal strut diameters in the range of 0.6-1.2 mm. Measured data was extrapolated with the linear function to show general trends. The percentage difference between the measured Gaussian and nominal diameters was concluded to decrease with increasing nominal diameters: 29% for 0.6 mm, 16% for 0.8 mm, 9% for 1.0 mm, and 4% for 1.2 mm. Based on the measurement results, the simulations with circular Gaussian and elliptical cross-sections were prepared for the remaining diameters equivalent to 0.6 mm, 1 mm, and 1.2 mm.

The results showed a good agreement between the experimental data and the numerical models that used elliptical geometry. Differences in terms of structure reaction forces were 29% for 0.6 mm, 6% for 1 mm, and 1% for 1.2 mm nominal diameter equivalent and deformation differences were 5% for 0.6 mm, 14% for 1 mm, and 5% for 1.2 mm nominal diameter equivalent. Bigger overall differences were observed for geometries that used circular cross-sections with Gaussian distribution. For reaction forces were 16% for 0.6 mm, 16% for 1 mm, and 14% for 1.2 mm nominal diameter equivalent and for deformations were 6% for 0.6 mm, 21% for 1 mm, and 23% for 1.2 mm nominal diameter equivalent. The last findings showed that the geometrical imperfections differed according to the strut diameter. It confirmed that the inclusion of manufacturing imperfections must be considered individually for each geometry, material and manufacturing setup. Furthermore, it showed that the inclusion of imperfections related to the shape and size of the cross-section can be sufficient to achieve accurate results.

6.2 Research paper II

The key findings of Research Paper II were related to the model of the material. The main aim was focused on the determination of material properties specific to thin struts of lattice structures and the assembly of the non-linear material model. The proposed workflow was based on the development of a special multi-strut tensile sample that was able to reflect conditions of lattice structure under loading. The course of elastic-plastic response of loaded samples gave a detailed overview of which mathematical equations were required for description of material behavior. The model developed for this purpose was adopted by simulations that used the solid and beam element model. Both types of simulations were further compared with the experiment and evaluated by several metrics.

The study focused on the BCC lattice structure made of 316L stainless steel using SLM technology. The nominal diameter of the strut changed in the range of 0.3-1.0 mm. In the first step, special multi-strut tensile samples were designed with a nominal strut diameter of 0.6 mm determined by the state of the art [18, 37]. In the next step, special samples were manufactured together with conventional samples and tested by quasi-static compression on the Zwick device.

The comparison of the different tensile samples showed a significant difference. Although the properties of conventional tensile samples (DIN 50125:2009-07, E=166±15 GPa, Ys=450±5 MPa) were comparable to the properties provided by SLM Solutions (DIN EN 10088:2014, ASTM A276, E=178 GPa, Ys=529 MPa, [116]), the multi-strut tensile samples showed a decrease (E=94±10 GPa, Ys=338±20 MPa). Further investigation of multi-strut samples showed a 49% lower Young's modulus compared to the single strut test with numerical corrections performed by Smith et al. [50]. In contrast, a comparison of the dual mode module described by Li et al. [27] showed an increase of approximately 30%. A good agreement of Young's modulus and other properties was achieved for the study by Gümrük et al. [26] who used similar samples. The wide range of properties can be explained by the different process parameters and geometry. These factors play an important role, especially in the production of thin-walled samples.

In the following step, the non-linear elastic-plastic material model based on the results of multi-strut tensile samples was adopted by numerical simulation. An optical digitization procedure similar to the previous study was performed to obtain manufacturing imperfections. Based on findings geometry models with circular Gaussian and elliptical cross-sections were prepared.

The first simulation considered only the linear elastic behavior of the material without including imperfections. For this setup, one solid element and two beam element models [33, 117] were compared with the experiment in terms of structure compressive modulus. One of the beam element models was prepared with modification of the nodal stiffness according to the Luxner study (1000 times higher Young's modulus) [33]. The radius of correction for stiffness in the near vicinity of the node was determined as a value of the nominal strut diameter +0.2 mm. The comparison showed that the compressive modulus of the structure without modifications was in good agreement with the experiment for all tested strut diameters (with an average error of 14%) [117]. In contrast to this, the beam element model with stiffness corrections was in good agreement with the experiment only for smaller strut diameters up to 0.6 mm. The compressive modulus then increased significantly. A similar behavior was observed for the solid element model, which was according to the expectations in compliance with beam element model that included stiffness corrections.

Then the non-linear behavior was included in the material model. For this setup four beam element models were compared: model with nominal geometry [117], model with nominal geometry and stiffness corrections [33], model with circle Gaussian cross-sections and stiffness corrections, and model with elliptical cross-sections and stiffness corrections. This time, both models with nominal geometry were shown to be consistent with the experiment in terms of compressive modulus (with average error 18% and 10%, respectively). On the other hand, models with modified cross-sections manifested higher stiffness compared to experimental values, especially for intermediate strut diameters (approx. twice in the range of 0.5-0.8 mm nominal diameter equivalent). It indicated that the different nominal cross-sections were influenced by the imperfections irregularly.

Three of these models were further compared with the experiment in the area of plastic deformations in terms of initial collapse stress, plateau stress at 30% strain, and volume energy absorbed up to 30% strain (see eqs. 2-18, 2-22, 2-28). The model with nominal geometry [117] appeared to have insufficient stiffness compared to the experiment. The lack of stiffness became significant with increasing strut diameter, and therefore the model was eliminated. Contrary to that, results closer to the experiment showed models with nodal stiffness modification and Gaussian, respectively, elliptical cross-section even for higher strut diameters. The most accurate results were achieved with elliptical cross-section and stiffness corrections, which confirmed findings from the previous study and justified the model of material developed in this research paper. Differences that occurred for simulations with larger strut diameters were caused by slightly different material properties for each diameter.

In the last step, a larger lattice structure was produced and tested in a similar way. Comparison of the experiment and the finite element analysis confirmed the functionality of the simulation using a non-linear model of the material based on multi-strut tensile samples with the inclusion of local modifications and geometrical imperfections (up to 11% difference in terms of stress at 0.3 strain).

6.3   Research paper III

The key findings of Research Paper III were related to the inclusion of dynamic loading effects in the material model. The study focused on the determination of the strain-rate sensitivity of the parent material for thin struts and its mathematical description. The proposed methodology workflow was based on the fast tensile test of multi-strut samples on a modified Hopkinson bars device. The result of this test quantified the differences between dynamic and quasi-static behavior determined in the previous study. Both series tested at different velocities were supplemented with data from other authors [18, 72, 73] and fitted with curves. According to the polynomial description of the curves, the most accurate input parameters of the constitutive C-S law were found. The material model containing this constitutive law was applied for simulations of lattice structure compression at different loading velocities.

In the paper several BCC and FCC based lattice structures made of stainless steel 316L with different parameters were investigated using experiment and FEM analysis of compression tests with different strain-rates. The governing nominal diameter was chosen at 0.6 mm for all struts, which led to a different volume fraction depending on the type of structure. Furthermore, the stand-alone struts were manufactured with different manufacturing angles, representing the angles of the struts in the structures. The struts were further digitized and geometry models were prepared based on measurement results similar to those of previous studies.

The results of the dynamic tensile test showed good agreement with three sets of C-S law parameters from the author that tested thin struts in a similar multi-strut composition [18]. The parameters sets in the original study were defined as 1 – up to 100 s^{-1} based on the yield stress; 2 – up to 6600 s^{-1} based on the yield stress; 4 – Estimation. All the mentioned sets were adopted by the material model and used in simulation performed at intermediate strain-rates (10^2-10^3 s^{-1}). The results compared to the experiment of six different structures in terms of initial collapse stress, plateau stress and SEA showed significant differences (see eqs. 2-18, 2-22, 2-28).

The initial collapse stress was consistent for parameter sets 1 and 2 but differed from the simulation with parameter set 4. Compared to the experiment, the simulation with parameters 1 and 2 was much closer to the average values of the experiment. On the other hand, when plateau stress and SEA were compared, parameter setup 4 showed better compliance with the experiment. However, the consistency of the simulations using setups 1 and 2 remained preserved.

In the next part, parameter set 4 was used for simulations of BCC lattice structure compression performed under different strain-rates. To compare them with the experiment, the data from quasi-static testing from the previous study had to be supplemented with intermediate and high loading rates (approx. $2.2 \cdot 10^3$ s^{-1}). The comparison of simulation and experiment in terms of initial collapse stress showed a relatively good agreement across the range of tested strain-rates. It showed that a similar approach can be used in the future for different structure topologies or process parameters.

7   CONCLUSIONS

This thesis focused on the development of non-linear computational model of lattice structures under different loading velocities with inclusion of geometrical imperfections. The most important issues were addressed to scientific questions identified based on the review of the literature.

The first part focused on determination of the effect of the most significant geometrical imperfections – change in strut cross-sectional shape and area. It was found that the nominal geometry did not fully represent the actual topology of the thin struts. Its use for the creation of geometry models in FEA led to distorted information about the deformation resistance and the deformation pattern. Therefore, the model was supplemented with the measured cross-sectional shape and diameter, which provided enough accurate results. The measured values were not universally applicable; however, a similar approach could be used for different topologies, parent materials or LPBF process parameters. The most important outputs were described as follows:

o   An optical digitization method revealed a 'water drop' shape of the strut cross-section.
o   The elliptic strut cross-section significantly increased the accuracy of the FEA compared to the Gaussian circular cross-section.
o   Partially melted powder particles on the strut surface caused a significant increase in structure weight.
o   Tensile tests showed the differences in the mechanical properties of the samples with angles of 90° and 45° with respect to the building platform.

The second part was focused on the correct determination of the input parameters of the non-linear material model that represented the properties of the lattice structure made of SS 316L. It was shown that conventional samples manufactured according to DIN standards were unable represent properties of thin-strut geometries. Furthermore, it was difficult to determine properties based on single strut. However, specially shaped samples that combined multiple struts and conventional samples in one multi-strut sample appeared to be suitable for this purpose. Moreover, the definition of the beam element model suffered from several simplifications. To improve its accuracy, the diameter of the strut in the near area of the nodes had to be increased by approximately 0.2 mm and the Young's modulus in this area had to be increased 1000 times. The approach had its limitations and did not allow to reflect behavior of a heavily deflected structure. The main conclusions of this part were described in the following points:

o   The test of specially shaped samples showed good agreement in properties compared to the literature dealing with similar multi-strut samples [18, 26]. Analytical models based on Euler-Bernoulli and Timoshenko beam theory [117] supported the credibility of mechanical properties in the linear-elastic area.

- o The determination of the mechanical properties for very thin struts had limitations. If the diameter of the struts changed a lot (<±0.3 mm), then the properties also changed.
- o Geometrical imperfections acquired different significance for different strut diameters. The most significant were for smaller strut diameters.
- o FE analyses using solid and beam element models predicted the compressive modulus of the lattice structure with similar accuracy if an increase in artificial stiffness in the vicinity of the nodes was used for the beam element model.
- o Including imperfections improved the accuracy of both FEM approaches beyond the yield point.
- o The powder particles partially melted on the surface of the structure had an important significance for the transmission of force. The finding was similar to the study by Vrana et al. [118], who determined geometrical imperfections for $AlSi_{10}Mg$ with similar methods.

The third part focused on the inclusion of an effect that caused a change in the material stress response under dynamic loading. The experimental findings of previous studies focused on dynamic loading of lattice structures were used and combined with the results of the Hopkinson tensile test of multi-strut samples. Based on this combination, the most suitable parameter setup was chosen. The model included the strain hardening represented by Hollomon and the C-S constitutive law, which modified the stress-strain response based on the strain rate. It was possible to use the model for various structure topologies considering the strut diameter similar to those used for multi-strut tensile samples. The biggest disadvantage was a limitation to a certain range of diameters. The main conclusions of this study were described in the following ways:

- o A good agreement of results obtained by the tensile tests of multi-strut samples and equations from the literature was found for a low strain-rate (approximately 220 s^{-1}).
- o The imperfections of the manufacturing process related to the variation in the strut cross-section could not be neglected.
- o The most efficient structure in terms of SEA was FCCz (average 0.39 $MJ \cdot m^{-3}$).
- o The consideration of different C-S input parameters led to different stress-strain responses at certain loading stages of the lattice structure.
- o The lack of contact between the struts in the beam element model appeared to be the main weakness of this approach.

Regarding the tested hypotheses, the obtained results are summarized in the following remarks:

Q1 How do geometric imperfections of the cross-sectional shape and size affect the compression response of the lattice structures with a nominal strut diameter in the range of 0.6-1.2 mm?

Computational analyzes that studied the effects of described imperfections showed a significant impact of their inclusion in the geometry model in the investigated range. Both contributed to an increase in the stiffness of the structure. Without their consideration, the resulting structure properties were underestimated in terms of deformation resistance. The influence of both types of imperfections was observed to decreased with increasing nominal strut diameter. The obtained results were valid only for specific ranges of diameters, material and process parameters set and could not be universally applied. Furthermore, some configurations tended to only mild non-circularities strut cross-section. Therefore, it had to be considered whether an elliptical approximation of the strut a cross-section was beneficial or if a circular cross-section was representative enough. In any case, reflecting imperfections related to the change in shape and size was beneficial and improved the accuracy of the simulation. **Thus, the first hypothesis was not falsified.**

Q2 How does the non-linear material model based on multi-strut tensile samples with stiffness corrections influence the deformation behavior of the lattice structure with nominal strut diameter in the range of 0.3-1.0 mm made of 316L stainless steel by SLM technology?

The tensile tests of specially shaped multi-strut samples achieved a more accurate resulting properties of lattice structures in comparison to the conventional samples. The non-linear elastic-plastic material model based on these results appeared to sufficiently represent the behavior of the lattice structure for loading beyond the yield point. The disadvantage of this approach was its limitation for a certain range of strut diameters. If the nominal strut diameter of the tensile sample differed significantly from the strut diameter of the lattice structure, then the resulting models suffered from significant inaccuracies. Furthermore, the material model used for the beam element model required additional local corrections in the near vicinity of the nodes. According to the compression test result, the range of material corrections and stiffness adjustments was identified. These corrections appeared to be significant in the area of plastic deformation, where they replaced the lack of beam connectivity. **Thus, the second hypothesis was not falsified.**

Q3 How does the implementation of strain-rate sensitivity into model of material influence the behavior of the 316L stainless steel lattice structure under dynamic compression loading in the range of 10^2-10^3 s^{-1} strain-rate?

It was proved that for the tested range of strain-rates, it was beneficial to include the effect of the sensitivity of the parent material on the strain-rate. Furthermore, the combination with deformation hardening in the form of linear or exponential dependence, appeared to be beneficial for accuracy of the simulation. Without strain-rate dependence, the simulation suffered from the decreased dynamic resistance. The difference was significant even for lower values of strain-rates (10^2 s^{-1}) as the stainless steel 316L showed a strong dependence on strain-rate sensitivity. **Thus, the third hypothesis was not falsified.**

8   LITERATURE

[1]   AHMAD, Zaini. *Impact and Energy Absorption of Empty and Foam-filled Conical Tubes*. 2009.

[2]   HUTCHINSON, John W. a Zhenyu XUE. *Metal sandwich plates optimized for pressure impulses* [online]. 2005. ISBN 0020-7403. doi:10.1016/j.ijmecsci.2004.10.012

[3]   DHARMASENA, Kumar P., H. N G WADLEY, Zhenyu XUE a John W. HUTCHINSON. Mechanical response of metallic honeycomb sandwich panel structures to high-intensity dynamic loading. *International Journal of Impact Engineering* [online]. 2008, **35**(9), 1063–1074. ISSN 0734743X. doi:10.1016/j.ijimpeng.2007.06.008

[4]   MOHMMED, Ramadan, Azzam AHMED, Mohamed Ahmed ELGALIB a Hashim ALI. Low Velocity Impact Properties of Foam Sandwich Composites : A Brief Review. *International Journal of Engineering Science and Innovative Technology (IJESIT)*. 2014, **3**(2), 579–591.

[5]   MOHMMED, Ramadan, Fa ZHANG, Baozhong SUN a Bohong GU. Finite element analyses of low-velocity impact damage of foam sandwiched composites with different ply angles face sheets. *Materials and Design* [online]. 2013, **47**, 189–199. ISSN 18734197. doi:10.1016/j.matdes.2012.12.016

[6]   LABEAS, G. N. a M. M. SUNARIC. Investigation on the static response and failure process of metallic open lattice cellular structures. *Strain* [online]. 2010. ISSN 00392103. doi:10.1111/j.1475-1305.2008.00498.x

[7]   WANG, Yonghui, Ximei ZHAI, Wenjian YING a Wei WANG. Dynamic crushing response of an energy absorption connector with curved plate and aluminum foam as energy absorber. *International Journal of Impact Engineering* [online]. 2018, **121**, 119–133. ISSN 0734743X. doi:10.1016/j.ijimpeng.2018.07.016

[8]   FANG, Dai Ning, Yu Long LI a Han ZHAO. *On the behaviour characterization of metallic cellular materials under impact loading* [online]. 2010. ISBN 0567-7718. doi:10.1007/s10409-010-0392-x

[9]   DESHPANDE, V. S. a N. A. FLECK. Isotropic constitutive models for metallic foams. *Journal of the Mechanics and Physics of Solids* [online]. 2000. ISSN 00225096. doi:10.1016/S0022-5096(99)00082-4

[10]   DESHPANDE, V. S., M. F. ASHBY a N. A. FLECK. Foam topology: Bending versus stretching dominated architectures. *Acta Materialia* [online]. 2001. ISSN 13596454. doi:10.1016/S1359-6454(00)00379-7

[11]   AHMAD, Z. a D. P. THAMBIRATNAM. Crushing response of foam-filled conical tubes under quasi-static axial loading. *Materials and Design* [online]. 2009, **30**(7), 2393–2403. ISSN 02641275. doi:10.1016/j.matdes.2008.10.017

[12]   BANHART, J. *Manufacture, characterisation and application of cellular metals and metal foams* [online]. 2001. ISBN 0079-6425. doi:10.1016/S0079-6425(00)00002-5

[13]   LABEAS, G a E PTOCHOS. Investigation of sandwich structures with innovative cellular metallic cores under low velocity impact loading. *Plastics, Rubber and Composites* [online]. 2013. ISSN 1465-8011. doi:10.1179/1743289811Y. 0000000056

[14] TANCOGNE-DEJEAN, Thomas, Adriaan B. SPIERINGS a Dirk MOHR. Additively-manufactured metallic micro-lattice materials for high specific energy absorption under static and dynamic loading. *Acta Materialia* [online]. 2016, **116**. ISSN 13596454. doi:10.1016/j.actamat.2016.05.054

[15] *ERG materials & aerospace* [online]. 2019. http://ergaerospace.com/applications/duocel-foam-energy-absorbers/

[16] MINES, R. A.W., S. TSOPANOS, Y. SHEN, R. HASAN a S. T. MCKOWN. Drop weight impact behaviour of sandwich panels with metallic micro lattice cores. *International Journal of Impact Engineering* [online]. 2013, **60**, 120–132. ISSN 0734743X. doi:10.1016/j.ijimpeng.2013.04.007

[17] TANCOGNE-DEJEAN, Thomas a Dirk MOHR. Stiffness and specific energy absorption of additively-manufactured metallic BCC metamaterials composed of tapered beams. *International Journal of Mechanical Sciences* [online]. 2018, **141**, 101–116. ISSN 00207403. doi:10.1016/j.ijmecsci.2018.03.027

[18] GÜMRÜK, Recep, R. A.W. MINES a Sami KARADENIZ. Determination of Strain Rate Sensitivity of Micro-struts Manufactured Using the Selective Laser Melting Method. *Journal of Materials Engineering and Performance* [online]. 2018, **27**(3), 1016–1032. ISSN 15441024. doi:10.1007/s11665-018-3208-y

[19] LABEAS, G. a Evangelos PTOCHOS. Homogenization of selective laser melting cellular material for impact performance simulation. *International Journal of Structural Integrity* [online]. 2015, **6**(4), 439–450. ISSN 17579872. doi:10.1108/IJSI-10-2014-0059

[20] HASAN, Rafidah, Robert A.W. MINES, E. SHEN, S. TSOPANOS, Wesley J. CANTWELL, W. BROOKS a C.J. SUTCLIFFE. Comparison of the Drop Weight Impact Performance of Sandwich Panels with Aluminium Honeycomb and Titanium Alloy Micro Lattice Cores. *Applied Mechanics and Materials* [online]. 2010, **24**–**25**, 413–418. ISSN 1662-7482. doi:10.4028/www.scientific.net/AMM.24-25.413

[21] USHIJIMA, K., W. J. CANTWELL, R. A.W. MINES, S. TSOPANOS a M. SMITH. An investigation into the compressive properties of stainless steel micro-lattice structures. *Journal of Sandwich Structures and Materials* [online]. 2011. ISSN 10996362. doi:10.1177/1099636210380997

[22] XIAO, Lijun a Weidong SONG. Additively-manufactured functionally graded Ti-6Al-4V lattice structures with high strength under static and dynamic loading: Experiments. *International Journal of Impact Engineering* [online]. 2018, **111**, 255–272. ISSN 0734743X. doi:10.1016/j.ijimpeng.2017.09.018

[23] CHEN, Zeyao, Zhe WANG, Shiwei ZHOU, Jianwang SHAO a Xian WU. Novel negative poisson's ratio lattice structures with enhanced stiffness and energy absorption capacity. *Materials* [online]. 2018, **11**(7). ISSN 19961944. doi:10.3390/ma11071095

[24] RADEK VRANA, ONDREJ VAVERKA, ONDREJ CERVINEK, LIBOR PANTELEJEV, JAKUB HURNIK, DANIEL KOUTNY, David Palousek. Heat Treatment of the SLM Processed Lattice Structure Made of AlSi10Mg and Its Effect on the Impact Energy Absorption. In: *Conference: Euro PM2019 Congress & Exhibition*. 2019, s. 6.

[25] OZDEMIR, Zuhal, Andrew TYAS, Russell GOODALL a Harm ASKES. Energy absorption in lattice structures in dynamics: Nonlinear FE simulations. *International Journal of Impact Engineering* [online]. 2017, **102**. ISSN 0734743X. doi:10.1016/j.ijimpeng.2016.11.016

[26] GÜMRÜK, R. a R. A W MINES. Compressive behaviour of stainless steel micro-lattice structures. *International Journal of Mechanical Sciences* [online]. 2013. ISSN 00207403. doi:10.1016/j.ijmecsci.2013.01.006

[27] LI, P., Z. WANG, N. PETRINIC a C. R. SIVIOUR. Deformation behaviour of stainless steel microlattice structures by selective laser melting. *Materials Science and Engineering A* [online]. 2014. ISSN 09215093. doi:10.1016/j.msea.2014.07.015

[28] WANG, Bing, Lin-Zhi WU, Li MA a Ji-Cai FENG. Low-velocity impact characteristics and residual tensile strength of carbon fiber composite lattice core sandwich structures. *Composites Part B: Engineering* [online]. 2011, **42**(4), 891–897. ISSN 13598368. doi:10.1016/j.compositesb.2011.01.007

[29] ŽMINDÁK, Milan, Zoran PELAGIĆ, Peter PASTOREK, Martin MOČILAN a Martin VYBOŠŤOK. Finite element modelling of high velocity impact on plate structures. In: *Procedia Engineering* [online]. 2016, s. 162–168. ISSN 18777058. doi:10.1016/j.proeng.2016.01.191

[30] MASKERY, I., N. T. ABOULKHAIR, A. O. AREMU, C. J. TUCK a I. A. ASHCROFT. Compressive failure modes and energy absorption in additively manufactured double gyroid lattices. *Additive Manufacturing* [online]. 2017, **16**. ISSN 22148604. doi:10.1016/j.addma.2017.04.003

[31] MASKERY, Ian, Alexandra HUSSEY, Ajit PANESAR, Adedeji AREMU, Christopher TUCK, Ian ASHCROFT a Richard HAGUE. An investigation into reinforced and functionally graded lattice structures. *Journal of Cellular Plastics* [online]. 2017. ISSN 15307999. doi:10.1177/0021955X16639035

[32] GRYTTEN, F., T. BØRVIK, O. S. HOPPERSTAD a M. LANGSETH. Low velocity perforation of AA5083-H116 aluminium plates. *International Journal of Impact Engineering* [online]. 2009, **36**(4), 597–610. ISSN 0734743X. doi:10.1016/j.ijimpeng.2008.09.002

[33] LUXNER, Mathias H., Juergen STAMPFL a Heinz E. PETTERMANN. Linear and nonlinear numerical investigations of regular open cell structures. In: *American Society of Mechanical Engineers, Aerospace Division (Publication) AD* [online]. 2004. ISSN 07334230. doi:10.1115/IMECE2004-62545

[34] LUXNER, Mathias H., Juergen STAMPFL a Heinz E. PETTERMANN. Finite element modeling concepts and linear analyses of 3D regular open cell structures. In: *Journal of Materials Science* [online]. 2005. ISSN 00222461. doi:10.1007/s10853-005-5020-y

[35] LUXNER, Mathias H., Alexander WOESZ, Juergen STAMPFL, Peter FRATZL a Heinz E. PETTERMANN. A finite element study on the effects of disorder in cellular structures. *Acta Biomaterialia* [online]. 2009. ISSN 17427061. doi:10.1016/j.actbio.2008.07.025

[36] KARAMOOZ RAVARI, M. R., M. KADKHODAEI, M. BADROSSAMAY a R. REZAEI. Numerical investigation on mechanical properties of cellular lattice structures fabricated by fused deposition modeling. *International Journal of Mechanical Sciences* [online]. 2014. ISSN 00207403. doi:10.1016/j.ijmecsci.2014.08.009

[37] DONG, Guoying a Yaoyao Fiona ZHAO. Numerical and experimental investigation of the joint stiffness in lattice structures fabricated by additive manufacturing. *International Journal of Mechanical Sciences* [online]. 2018. ISSN 00207403. doi:10.1016/j.ijmecsci.2018.09.014

[38] GENG, Xiaoliang, Liyang MA, Chao LIU, Chen ZHAO a Zhu Feng YUE. A FEM study on mechanical behavior of cellular lattice materials based on combined elements. *Materials Science and Engineering A* [online]. 2018. ISSN 09215093. doi:10.1016/j.msea.2017.11.082

[39] GIBSON, Lorna J. a Michael F. ASHBY. *Cellular solids: Structure and properties, second edition* [online]. 2014. ISBN 9781139878326. doi:10.1017/CBO9781139878326

[40] LEI, Hongshuai, Chuanlei LI, Jinxin MENG, Hao ZHOU, Yabo LIU, Xiaoyu ZHANG, Panding WANG a Daining FANG. Evaluation of compressive properties of SLM-fabricated multi-layer lattice structures by experimental test and μ-CT-based finite element analysis. *Materials and Design* [online]. 2019. ISSN 18734197. doi:10.1016/j.matdes.2019.107685

[41] YAN, Chunze, Liang HAO, Ahmed HUSSEIN, Philippe YOUNG a David RAYMONT. Advanced lightweight 316L stainless steel cellular lattice structures fabricated via selective laser melting. *Materials and Design* [online]. 2014. ISSN 18734197. doi:10.1016/j.matdes.2013.10.027

[42] KOUTNY, Daniel, Radek VRANA a David PALOUSEK. Dimensional accuracy of single beams of AlSi10Mg alloy and 316L stainless steel manufactured by SLM. In: *5th International Conference on Additive Technologies iCAT2014*. 2014. ISBN 978-961-281-579-0.

[43] LIU, Lu, Paul KAMM, Francisco GARCÍA-MORENO, John BANHART a Damiano PASINI. Elastic and failure response of imperfect three-dimensional metallic lattices: the role of geometric defects induced by Selective Laser Melting. *Journal of the Mechanics and Physics of Solids* [online]. 2017. ISSN 00225096. doi:10.1016/j.jmps.2017.07.003

[44] LIU, Yabo, Zhichao DONG, Jun LIANG a Jingran GE. Determination of the strength of a multilayer BCC lattice structure with face sheets. *International Journal of Mechanical Sciences* [online]. 2019. ISSN 00207403. doi:10.1016/j.ijmecsci.2019.01.026

[45] SIMULIA, Dassault Systèmes. Abaqus 6.14 / Analysis User's Guide. *ABAQUS 6.14 Analysis User's Guide* [online]. 2014, **I**, 862. ISSN 1098-6596. doi:10.1017/CBO9781107415324.004

[46] BECKER, Roland a Boris VEXLER. Mesh refinement and numerical sensitivity analysis for parameter calibration of partial differential equations. *Journal of Computational Physics* [online]. 2005. ISSN 10902716. doi:10.1016/j.jcp.2004.12.018

[47] HALLQUIST, Jo. *LS-DYNA® theory manual*. 2006. ISBN 9254492507.

[48] LOZANOVSKI, Bill, Martin LEARY, Phuong TRAN, Darpan SHIDID, Ma QIAN, Peter CHOONG a Milan BRANDT. Computational modelling of strut defects in SLM manufactured lattice structures. *Materials and Design* [online]. 2019. ISSN 18734197. doi:10.1016/j.matdes.2019.107671

[49] YADROITSEV, I. a I. SMUROV. Selective laser melting technology: From the single laser melted track stability to 3D parts of complex shape. In: *Physics Procedia* [online]. 2010. ISBN 18753892. doi:10.1016/j.phpro.2010.08.083

[50] SMITH, M., Z. GUAN a W. J. CANTWELL. Finite element modelling of the compressive response of lattice structures manufactured using the selective laser melting technique. *International Journal of Mechanical Sciences* [online]. 2013, **67**, 28–41. ISSN 00207403. doi:10.1016/j.ijmecsci.2012.12.004

[51] MINES, Robert A.W., Sozohn TSOPANOS a S.T. MCKOWN. Verification of a Finite Element Simulation of the Progressive Collapse of Micro Lattice Structures. *Applied Mechanics and Materials* [online]. 2011, **70**, 111–116. ISSN 1662-7482. doi:10.4028/www.scientific.net/AMM.70.111

[52] TSOPANOS, S., R. A.W. MINES, S. MCKOWN, Y. SHEN, W. J. CANTWELL, W. BROOKS a C. J. SUTCLIFFE. The influence of processing parameters on the mechanical properties of selectively laser melted stainless steel microlattice structures. *Journal of Manufacturing Science and Engineering, Transactions of the ASME* [online]. 2010, **132**(4), 0410111–04101112. ISSN 10871357. doi:10.1115/1.4001743

[53] CHAWLA, N. a X. DENG. Microstructure and mechanical behavior of porous sintered steels. *Materials Science and Engineering A* [online]. 2005. ISSN 09215093. doi:10.1016/j.msea.2004.08.046

[54] LI, Chuanlei, Hongshuai LEI, Yabo LIU, Xiaoyu ZHANG, Jian XIONG, Hao ZHOU a Daining FANG. Crushing behavior of multi-layer metal lattice panel fabricated by selective laser melting. *International Journal of Mechanical Sciences* [online]. 2018. ISSN 00207403. doi:10.1016/j.ijmecsci.2018.07.029

[55] CHEN, Liming, Jian ZHANG, Bing DU, Hao ZHOU, Houchang LIU, Yongguang GUO, Weiguo LI a Daining FANG. Dynamic crushing behavior and energy absorption of graded lattice cylindrical structure under axial impact load. *Thin-Walled Structures* [online]. 2018, **127**, 333–343. ISSN 02638231. doi:10.1016/j.tws.2017.10.048

[56] SILVA, Matthew J. a Lorna J. GIBSON. The effects of non-periodic microstructure and defects on the compressive strength of two-dimensional cellular solids. *International Journal of Mechanical Sciences* [online]. 1997. ISSN 00207403. doi:10.1016/s0020-7403(96)00065-3

[57] LI, Xin, Peiwen ZHANG, Zhihua WANG, Guiying WU a Longmao ZHAO. Dynamic behavior of aluminum honeycomb sandwich panels under air blast: Experiment and numerical analysis. *Composite Structures* [online]. 2014, **108**(1), 1001–1008. ISSN 02638223. doi:10.1016/j.compstruct.2013.10.034

[58] MINES, R. A. W., S. MCKOWN, W. CANTWELL, W. BROOKS a C. J. SUTCLIFFE. On the Progressive Collapse of Micro Lattice Structures. In: *Experimental Analysis of Nano and Engineering Materials and Structures* [online]. 2007. doi:10.1007/978-1-4020-6239-1_369

[59] HARRIS, J. A., R. E. WINTER a G. J. MCSHANE. Impact response of additively manufactured metallic hybrid lattice materials. *International Journal of Impact Engineering* [online]. 2017, **104**, 177–191. ISSN 0734743X. doi:10.1016/j.ijimpeng.2017.02.007

[60] J., Hollomon. Properties and structure of steel - tensile deformation. *AIME Trans*. 1945, **162**(268), 90.

[61] P., Ludwik. Elemente der technologischen mechanik. *Julius Springer*. 1909.

[62] E., Voce. A practical strain hardening function. *Metallurgia*. 1955, **91**(219).

[63] LUDWIGSON, D. C. Modified stress-strain relation for FCC metals and alloys. *Metallurgical Transactions* [online]. 1971. ISSN 03602133. doi:10.1007/BF02813258

[64] AMANI, Yasin, Sylvain DANCETTE, Pauline DELROISSE, Aude SIMAR a Eric MAIRE. Compression behavior of lattice structures produced by selective laser melting: X-ray tomography based experimental and finite element approaches. *Acta Materialia* [online]. 2018. ISSN 13596454. doi:10.1016/j.actamat.2018.08.030

[65] TVERGAARD, V. a A. NEEDLEMAN. Analysis of the cup-cone fracture in a round tensile bar. *Acta Metallurgica* [online]. 1984. ISSN 00016160. doi:10.1016/0001-6160(84)90213-X

[66] CHU, C. C. a A. NEEDLEMAN. Void nucleation effects in biaxially stretched sheets. *Journal of Engineering Materials and Technology, Transactions of the ASME* [online]. 1980. ISSN 15288889. doi:10.1115/1.3224807

[67] *Abaqus Version 6.13 Documentation Collection*. 2013.

[68] ŠLAIS, Miroslav. *Studium vlivu rychlostních a teplotních parametrů na tvařitelnost Ti slitin*. B.m., 2012. Vysoké učení technické v Brně.

[69] WANG, Xuemei a Jun SHI. Validation of Johnson-Cook plasticity and damage model using impact experiment. *International Journal of Impact Engineering* [online]. 2013. ISSN 0734743X. doi:10.1016/j.ijimpeng.2013.04.010

[70] DIETENBERGER, Michael, Murat BUYUK a Cing-Dao(Steve) KAN. Development of a high strain-rate dependent vehicle model. *LS-Dyna Anwenderforum*. 2005.

[71] KADHANE, Somnath a Hemant WARHATKAR. Review of Experimental Techniques used to Study the Mechanical Behaviour of Biological Soft Tissues. In: [online]. 2017. doi:10.2991/iccasp-16.2017.44

[72] LANGDON, G. S. a G. K. SCHLEYER. Unusual strain rate sensitive behaviour of AISI 316L austenitic stainless steel. *Journal of Strain Analysis for Engineering Design* [online]. 2004. ISSN 03093247. doi:10.1177/030932470403900106

[73] BURGAN, B. *Elevated temperature and high strain rate properties of offshore steels*. 2001. ISBN 0 7176 2023 9.

[74] NOLTING, A. E., R. ARSENAULT a M. BOLDUC. Increased accuracy of SHPB test apparatus to better evaluate naval steels. In: *Procedia Engineering* [online]. 2011. ISSN 18777058. doi:10.1016/j.proeng.2011.04.375

[75] YOUNG, Kevin. Development of a Tensile Split Hopkinson Pressure Bar Testing Facility. *Eletronic Theses and Dissertations*. 2015.

[76] MINES, R. A.W., S. MCKOWN, S. TSOPANOS, E. SHEN, W. CANTWELL, W. BROOKS a C. SUTCIIFFE. Local effects during indentation of fully supported sandwich panels with micro lattice cores. In: *Applied Mechanics and Materials* [online]. 2008. ISSN 16627482. doi:10.4028/www.scientific.net/AMM.13-14.85

[77] *Data sheet: CTIII-1/4 -5056-0.001N-2.3*. 2012.

[78] MCKOWN, S., Y. SHEN, W. K. BROOKES, C. J. SUTCLIFFE, W. J. CANTWELL, G. S. LANGDON, G. N. NURICK a M. D. THEOBALD. The quasi-static and blast loading response of lattice structures. *International Journal of Impact Engineering* [online]. 2008. ISSN 0734743X. doi:10.1016/j.ijimpeng.2007.10.005

[79] ASHBY, MF, A EVANS, NA FLECK, LJ GIBSON, JW HUTCHINSON, HNG WADLEY, a F DELALE,. Metal Foams: A Design Guide. *Applied Mechanics Reviews* [online]. 2001. ISSN 0003-6900. doi:10.1115/1.1421119

[80] WINTER, R. E., M. COTTON, E. J. HARRIS, D. J. CHAPMAN, D. EAKINS a G. MCSHANE. Plate-impact loading of cellular structures formed by selective laser melting. In: *WIT Transactions on the Built Environment* [online]. 2012, s. 145–156. ISBN 17433509. doi:10.2495/SU120131

[81] RADFORD, D. D., G. J. MCSHANE, V. S. DESHPANDE a N. A. FLECK. Dynamic compressive response of stainless-steel square honeycombs. *Journal of Applied Mechanics, Transactions ASME* [online]. 2007. ISSN 00218936. doi:10.1115/1.2424717

[82] CAO, Xiaofei, Dengbao XIAO, Ying LI, Weibin WEN, Tian ZHAO, Zihao CHEN, Yongbo JIANG a Daining FANG. Dynamic compressive behavior of a modified additively manufactured rhombic dodecahedron 316L stainless steel lattice structure. *Thin-Walled Structures* [online]. 2020. ISSN 02638231. doi:10.1016/j.tws.2019.106586

[83] XIAO, Lijun, Weidong SONG a Xiao XU. Experimental study on the collapse behavior of graded Ti-6Al-4V micro-lattice structures printed by selective laser melting under high speed impact. *Thin-Walled Structures* [online]. 2020. ISSN 02638231. doi:10.1016/j.tws.2020.106970

[84] GIBSON, L.J. a M.F. ASHBY. Cellular Solids: Structure & Properties. *Advances in Polymer Technology*. 1989. ISSN 1365-2850.

[85] L. J. GIBSON, M. F. Ashby. Cellular Solids: Structure and Properties, 2d ed. *Cambridge University Press*. 1997.

[86] OZDEMIR, Zuhal, Everth HERNANDEZ-NAVA, Andrew TYAS, James A. WARREN, Stephen D. FAY, Russell GOODALL, Iain TODD a Harm ASKES. Energy absorption in lattice structures in dynamics: Experiments. *International Journal of Impact Engineering* [online]. 2016. ISSN 0734743X. doi:10.1016/j.ijimpeng.2015.10.007

[87] ZHAO, Miao, Fei LIU, Guang FU, David ZHANG, Tao ZHANG a Hailun ZHOU. Improved Mechanical Properties and Energy Absorption of BCC Lattice Structures with Triply Periodic Minimal Surfaces Fabricated by SLM. *Materials* [online]. 2018, **11**(12), 2411. ISSN 1996-1944. doi:10.3390/ma11122411

[88] ZHANG, Lei, Stefanie FEIH, Stephen DAYNES, Shuai CHANG, Michael Yu WANG, Jun WEI a Wen Feng LU. Energy absorption characteristics of metallic triply periodic minimal surface sheet structures under compressive loading. *Additive Manufacturing* [online]. 2018. ISSN 22148604. doi:10.1016/j.addma.2018.08.007

[89] LI, Dawei, Wenhe LIAO, Ning DAI, Guoying DONG, Yunlong TANG a Yi Min XIE. Optimal design and modeling of gyroid-based functionally graded cellular structures for additive manufacturing. *CAD Computer Aided Design* [online]. 2018. ISSN 00104485. doi:10.1016/j.cad.2018.06.003

[90] INTERNATIONAL ORGANIZATION FOR STANDARDIZATION. Mechanical testing of metals – Ductility testing – Compression test for porous and cellular metals. *International Organization for Standardization*. 2011.

[91] LUXNER, Mathias H., Juergen STAMPFL a Heinz E. PETTERMANN. Numerical simulations of 3D open cell structures - influence of structural irregularities on elasto-plasticity and deformation localization. *International Journal of Solids and Structures* [online]. 2007. ISSN 00207683. doi:10.1016/j.ijsolstr.2006.08.039

[92] YAN, Chunze, Liang HAO, Ahmed HUSSEIN, Simon Lawrence BUBB, Philippe YOUNG a David RAYMONT. Evaluation of light-weight AlSi10Mg periodic cellular lattice structures fabricated via direct metal laser sintering. *Journal of Materials Processing Technology* [online]. 2014, **214**(4). ISSN 09240136. doi:10.1016/j.jmatprotec.2013.12.004

[93] MATACHE, L. C., P. LIXANDRU, T. CHERECHES, A. MAZURU, D. CHERECHES, V. GEANTA, I. VOICULESCU, E. TRANA a A. N. ROTARIU. Determination of material constants for high strain rate constitutive model of high entropy alloys. In: *IOP Conference Series: Materials Science and Engineering* [online]. 2019. ISSN 1757899X. doi:10.1088/1757-899X/591/1/012057

[94] BANERJEE, A., S. DHAR, S. ACHARYYA, D. DATTA a N. NAYAK. Determination of Johnson cook material and failure model constants and numerical modelling of Charpy impact test of armour steel. *Materials Science and Engineering A* [online]. 2015. ISSN 09215093. doi:10.1016/j.msea.2015.05.073

[95] 2020 ERG AEROSPACE CORP. *ERG materials and aerospace* [online]. Dostupné z: http://ergaerospace.com/technical-data/duocel-foam-energy-absorption/

[96] WANG, Yonghui, J. Y.Richard LIEW, Siew Chin LEE a Wei WANG. Experimental and analytical studies of a novel aluminum foam filled energy absorption connector under quasi-static compression loading. *Engineering Structures* [online]. 2017. ISSN 18737323. doi:10.1016/j.engstruct.2016.10.020

[97] ZHANG, Pan, Yuansheng CHENG, Jun LIU, Yong LI, Changzai ZHANG, Hailiang HOU a Chunming WANG. Experimental study on the dynamic response of foam-filled corrugated core sandwich panels subjected to air blast loading. *Composites Part B: Engineering* [online]. 2016, **105**. ISSN 13598368. doi:10.1016/j.compositesb.2016.08.038

[98] MASKERY, I., C. TUCK, A.O. AREMU, I. MASKERY, C. TUCK, I.A. ASHCROFT, R.D. WILDMAN a R.I.M HAGUE. A comparative Finite Element study of cubic unit cells for Selective Laser Melting. *International Solid Freeform Fabrication Symposium2*. 2014, 1238–1249.

[99] VRÁNA RADEK, KOUTNÝ DANIEL, PALOUŠEK DAVID, Zikmund Tomáš. Influence of Selective Laser Melting Process Parameters on Impact Resistance of Lattice Structure made from AlSi10Mg. 2016, 6.

[100] QIU, Chunlei, Sheng YUE, Nicholas J.E. ADKINS, Mark WARD, Hany HASSANIN, Peter D. LEE, Philip J. WITHERS a Moataz M. ATTALLAH. Influence of processing conditions on strut structure and compressive properties of cellular lattice structures fabricated by selective laser melting. *Materials Science and Engineering A* [online]. 2015. ISSN 09215093. doi:10.1016/j.msea.2015.01.031

[101] PYKA, Grzegorz, Greet KERCKHOFS, Ioannis PAPANTONIOU, Mathew SPEIRS, Jan SCHROOTEN a Martine WEVERS. Surface Roughness and Morphology Customization of Additive Manufactured Open Porous Ti6Al4V Structures [online]. 2013, 4737–4757. doi:10.3390/ma6104737

[102] PYKA, Grzegorz, Greet KERCKHOFS, Jan SCHROOTEN a Martine WEVERS. The effect of spatial micro-CT image resolution and surface complexity on the morphological 3D analysis of open porous structures. *Materials Characterization* [online]. 2014, **87**. ISSN 10455803. doi:10.1016/j.matchar.2013.11.004

[103] RASHED, M. G., Mahmud ASHRAF, R. A.W. MINES a Paul J. HAZELL. Metallic microlattice materials: A current state of the art on manufacturing, mechanical properties and applications. *Materials and Design* [online]. 2016. ISSN 18734197. doi:10.1016/j.matdes.2016.01.146

[104] FÍLA, Tomáš, Petr KOUDELKA, Jan FALTA, Petr ZLÁMAL, Václav RADA, Marcel ADORNA, Stefan BRONDER a Ondřej JIROUŠEK. Dynamic impact testing of cellular solids and lattice structures: Application of two-sided direct impact Hopkinson bar. *International Journal of Impact Engineering* [online]. 2021. ISSN 0734743X. doi:10.1016/j.ijimpeng.2020.103767

[105] VRÁNA, R. *Návrh porézních struktur pro aditivní výrobu technologií selective laser melting*. B.m., 2014. Vysoké učení technické v Brně.

[106] BREMEN, Sebastian, Wilhelm MEINERS a Andrei DIATLOV. Selective Laser Melting A manufacturing technology for the future? *Laser Technik Journal* [online]. 2012. ISSN 16137728. doi:10.1002/latj.201290018

[107] ČIŽMÁROVÁ, Elena a Jana SOBOTOVÁ. *Nauka o materiálu I. a II.: cvičení*. Praha: České vysoké učení technické, 2014. ISBN 978-80-01-05550-2.

[108] THIJS, Lore, Karolien KEMPEN, Jean Pierre KRUTH a Jan VAN HUMBEECK. Fine-structured aluminium products with controllable texture by selective laser melting of pre-alloyed AlSi10Mg powder. *Acta Materialia* [online]. 2013, **61**(5), 1809–1819. ISSN 13596454. doi:10.1016/j.actamat.2012.11.052

[109] PALOUSEK, David, Milan OMASTA, Daniel KOUTNY, Josef BEDNAR, Tomas KOUTECKY a Filip DOKOUPIL. Effect of matte coating on 3D optical measurement accuracy. *Optical Materials* [online]. 2015. ISSN 09253467. doi:10.1016/j.optmat.2014.11.020

[110] URBÁNEK, Aleš. *Kontrola součástí pomocí metod reverzního inženýrství: Bakalářská práce*. B.m., 2008. Vysoké učení technické v Brně.

[111] ČERMÁK, Jan. Metody 3D skenování objektů. *B.m.* 2015.

[112] YAHAYA, M. A., D. RUAN, G. LU a M. S. DARGUSCH. Response of aluminium honeycomb sandwich panels subjected to foam projectile impact - An experimental study. *International Journal of Impact Engineering* [online]. 2015, **75**, 100–109. ISSN 0734743X. doi:10.1016/j.ijimpeng.2014.07.019

[113] AHMAD, Z., D. P. THAMBIRATNAM a A. C C TAN. Dynamic energy absorption characteristics of foam-filled conical tubes under oblique impact loading. *International Journal of Impact Engineering* [online]. 2010, **37**(5), 475–488. ISSN 0734743X. doi:10.1016/j.ijimpeng.2009.11.010

[114] VRANA, RADEK, Daniel KOUTNY a David PALOUSEK. IMPACT RESISTANCE OF DIFFERENT TYPES OF LATTICE STRUCTURES MANUFACTURED BY SLM. *MM Science Journal* [online]. 2016, (06), 1579–1585. doi:10.17973/MMSJ.2016_12_2016186

[115] VRANA, R., D. KOUTNY, D. PALOUSEK a T. ZIKMUND. Impact resistance of lattice structure made by selective laser melting from AlSi12 alloy. *MM Science Journal* [online]. 2015, **2015**(DECEMBER), 849–852. ISSN 18050476 18031269. doi:10.17973/MMSJ.2015_12_201547

[116] SHEET, Material Data. Material daten blatt. nedatováno.

[117] YANG, Yunhui, Meijuan SHAN, Libin ZHAO, Dexuan QI a Jianyu ZHANG. Multiple strut-deformation patterns based analytical elastic modulus of sandwich BCC lattices. *Materials and Design* [online]. 2019. ISSN 18734197. doi:10.1016/j.matdes.2019.107916

[118] VRÁNA, Radek, Daniel KOUTNÝ, David PALOUŠEK, Libor PANTĚLEJEV, Jan JAROŠ, Tomáš ZIKMUND a Jozef KAISER. Selective Laser Melting Strategy for Fabrication of Thin Struts Usable in Lattice Structures. *Materials* [online]. 2018. doi:10.3390/ma11091763

AUTHOR'S PUBLICATIONS

8.1 Papers published in journals with impact factor

VRÁNA, R.; ČERVINEK, O.; MAŇAS, P.; KOUTNÝ, D.; PALOUŠEK, D. Dynamic Loading of Lattice Structure Made by Selective Laser Melting-Numerical Model with Substitution of Geometrical Imperfections, 2018, vol. 11, no. 11, p. 1-22. ISSN 1996-1944

ČERVINEK, O.; WERNER, B.; KOUTNÝ, D.; VAVERKA, O.; PANTĚLEJEV, L.; PALOUŠEK, D. Computational Approaches of Quasi-Static Compression Loading of SS316L Lattice Structures Made by Selective Laser Melting. Materials, 2021, vol. 14, no. 9, p. 1-24. ISSN: 1996-1944.

WERNER, B.; ČERVINEK, O.; KOUTNÝ, D.; REISINGER, A.; PETTERMANN, H.E.; TODT, M. Numerical and experimental study on the collapse of a triangular cell under. International Journal of Solids and Structures, 2021, vol. 236, no. 76, p. 1-12. ISSN: 0020-7683.

ČERVINEK, O.; PETTERMANN, H.; TODT, M.; KOUTNÝ, D.; VAVERKA, O. Non-linear dynamic finite element analysis of micro-strut lattice structures made by laser powder bed fusion. Journal of Materials Research and Technology, 2022, vol. 18, no. 1-16, p. 3684-3699. ISSN: 2238-7854.

VRÁNA, R.; KOUTECKÝ, T.; ČERVINEK, O.; ZIKMUND, T.; PANTĚLEJEV, L.; KAISER, J.; KOUTNÝ, D. Deviations of the SLM produced Lattice Structures and Their Influence on Mechanical properties. Materials, 2022, vol. 15, no. 9, p. 1-20. ISSN: 1996-1944.

8.2 Papers in conference proceedings

VRÁNA, R.; VAVERKA, O.; ČERVINEK, O.; PANTĚLEJEV, L.; HURNÍK, J.; KOUTNÝ, D.; PALOUŠEK, D. Heat Treatment of the SLM Processed Lattice Structure Made of AlSi10Mg and Its Effect on the Impact Energy Absorption

ČERVINEK, O.; VRÁNA, R. KOUTNÝ, D.; PALOUŠEK, D. Static and Dynamic Compression Performance of Lattice Structures Made by Selective Laser Melting.

8.3 Other results

functional specimen (RIV-G/B) – Protective element based on energy absorption

CURRICULUM VITAE

Ing. Ondřej Červinek
Date of birth: 15/10/1993

Education

o 2018 – 2022 Doctoral study at Institute of Machine and Industrial Design, BUT. Topic: *Computational models for non-linear mechanical loading analyses of lattice structure made by laser powder bed fusion.*
o 2016 – 2018 Master study at Institute of Machine and Industrial Design, BUT. Topic: *Numerical model of lattice structure under dynamic loading made by selective laser melting technology.*
o 2013 – 2016 Bachelor study at Faculty of Mechanical Engineering, BUT. Topic: *3D lattice structures for application in selective laser melting technology.*

Honours & Awards

o 2nd place in Student competition SVS FEM of best ANSYS project (Prof. Jaroslav Buchar Award) – SVS FEM s.r.o.
o Winner of Diploma theses conference – BUT FEM
o Rector's Commemorative Medal of Merit – BUT

Teaching activities – seminars

o Teaching in Bachelor's programme – Design and CAD, Machine Design, Machine design fundamentals, CAD - Basic
o Teaching in Master's programme – 3D Digital Technology and CAD, Analytical Project, FEM-Advanced Analyses, Additive technologies, FEM-Structural Analyses
o Supervision of theses – Bachelor theses, Master theses

Participation in scientific projects

o 2016 – 2017, ESA Contract. Design of Spacecraft Components for Additive Manufacturing, ESA Czech Industry Incentive Scheme AO /1-7397/13/NL/EL
o 2017 – 2019. FSI-S-17-4144: Development of process parameters of selective laser melting technology for the production of unique metal parts
o 2017 – 2020, ESA Contract no. 4000123317/18/NL/GLC/hh, Additive Design for Aerospace Applications Capabilities (ADAAC), team member
o 2018 – 2022, OP VVV: CZ.02.1.01/0.0/0.0/16_025/0007304. ARMADIT, Materials with an internal architecture structures for additive technologies

Internships

o Guest researcher (1/6/2021 – 31/8/2021) – Institute of Lightweight Design and Structural Biomechanics, TU Wien
o Guest researcher (1/2/2022 – 31/7/2022) – Institute of Virtual Manufacturing, ETH Zürich

Language skills

o Czech, English (B2), German (A1)

Expertise

o 3D optical digitization and measurement, Non-linear structural finite element analysis, Additive manufacturing, Selective Laser Melting - SLM280hl, EOS400, Rapid prototyping and additive technologies, CAD softwares - Autodesk, Dassault Systemes, Explicit dynamic finite element analysis

ABSTRACT

The development of additive technologies has enabled the manufacturing of lightweight lattice structures with mechanical energy absorption potential. Their implementation in vehicle deformation zones can increase the safety of passengers. For their effective application the specific properties and deformation characteristics of lattice structures must be accurately mathematically described. However, a mathematical model that would consider a description of all significant deformation characteristics of lattice structures is not available. Therefore, this thesis focuses on development of non-linear numerical model of lattice structures loading with inclusion of the most significant geometrical imperfections, specific properties of multi-strut samples and dynamic effects. The structures are made of aluminum alloy AlSi$_{10}$Mg and stainless steel 316L using the selective laser melting technology. Two different finite element analysis approaches are used to create the geometry model that allows inspection of the deformation features in detail. The results of both models confirm that geometrical imperfections related to a change in shape and cross-sectional area of the strut have a significant impact on the mechanical properties. Furthermore, the mechanical properties of lattice structures determined by multi-strut samples significantly better represent properties of structures for quasi-static and dynamic loading. The final parameter verification simulation of lattice structures loading at several velocities shows good agreement between the experiment and the computational solution.

ABSTRAKT

Rozvoj aditivních technologií umožnil výrobu odlehčených mikro-prutových struktur s potenciálem v oblasti absorpce mechanické energie. Jejich implementací do deformačních zón vozidel může být docíleno zvýšení bezpečnosti posádky. Pro jejich efektivní využití je zapotřebí matematicky přesně popsat specifické vlastnosti a deformační charakteristiky mikro-prutových struktur. Nicméně matematický model, který by zahrnoval popis všech významných charakteristik deformace mikro-prutových struktur, není k dispozici. Proto se tato práce zaměřuje na vývoj nelineárního numerického modelu zatěžování mikro-prutových struktur se zahrnutím efektů spojených s nejvýznamnějšími geometrickými imperfekcemi, specifickými vlastnostmi multi-prutových vzorků a dynamickými efekty. Struktury jsou vyrobeny z hliníkové slitiny AlSi$_{10}$Mg a nerezové oceli 316L s využitím technologie selektivního laserového tavení. Dva odlišné přístupy jsou použity k vytvoření modelu geometrie, což umožňuje detailní inspekci deformačního charakteru. Výsledky obou modelů potvrzují, že geometrické imperfekce spojené se změnou tvaru a velikosti průřezu prutu mají významný vliv na mechanické vlastnosti. Navíc mechanické vlastnosti mikro-prutových struktur stanovené pomocí multi-prutových vzorků výrazně lépe reprezentují vlastnosti struktur pro kvazistatické i dynamické zatěžování. Finální parametrická ověřovací simulace zatěžování mikro-prutové struktury při několika rychlostech ukazuje dobrou shodu experimentu a výpočtového řešení.